

University of Windsor

Scholarship at UWindor

Electronic Theses and Dissertations

Theses, Dissertations, and Major Papers

2013

Synthesis and Characterisation of N-Heterocyclic Carbene Adducts of PI Cations

Ala'aeddeen Swidan
University of Windsor

Follow this and additional works at: <https://scholar.uwindsor.ca/etd>

Recommended Citation

Swidan, Ala'aeddeen, "Synthesis and Characterisation of N-Heterocyclic Carbene Adducts of PI Cations" (2013). *Electronic Theses and Dissertations*. 5000.
<https://scholar.uwindsor.ca/etd/5000>

This online database contains the full-text of PhD dissertations and Masters' theses of University of Windsor students from 1954 forward. These documents are made available for personal study and research purposes only, in accordance with the Canadian Copyright Act and the Creative Commons license—CC BY-NC-ND (Attribution, Non-Commercial, No Derivative Works). Under this license, works must always be attributed to the copyright holder (original author), cannot be used for any commercial purposes, and may not be altered. Any other use would require the permission of the copyright holder. Students may inquire about withdrawing their dissertation and/or thesis from this database. For additional inquiries, please contact the repository administrator via email (scholarship@uwindsor.ca) or by telephone at 519-253-3000ext. 3208.

Synthesis and Characterisation of *N*-Heterocyclic Carbene Adducts of P^I Cations

By

Ala'aeddeen Swidan

A Thesis
submitted to the Faculty of Graduate Studies
through the Department of Chemistry and Biochemistry
in Partial Fulfillment of the Requirements for
the Degree of Masters of Science
at the University of Windsor

Windsor, Ontario, Canada

2013

© 2013 Ala'aeddeen Swidan

Synthesis and Characterisation of *N*-Heterocyclic Carbene Adducts of P^I Cations

by

Ala'aeddeen Swidan

APPROVED BY:

Dr. W. Kedzierski
Department of Physics

Dr. S. Holger Eichhorn
Department of Chemistry and Biochemistry

Dr. Charles L. B. Maconald
Department of Chemistry and Biochemistry

Declaration of Originality

I hereby certify that I am the sole author of this thesis and that no part of this thesis has been published or submitted for publication.

I certify that, to the best of my knowledge, my thesis does not infringe upon anyone's copyright nor violate any proprietary rights and that any ideas, techniques, quotations, or any other material from the work of other people included in my thesis, published or otherwise, are fully acknowledged in accordance with the standard referencing practices. Furthermore, to the extent that I have included copyrighted material that surpasses the bounds of fair dealing within the meaning of the Canada Copyright Act, I certify that I have obtained a written permission from the copyright owner(s) to include such material(s) in my thesis and have included copies of such copyright clearances to my appendix.

I declare that this is a true copy of my thesis, including any final revisions, as approved by my thesis committee and the Graduate Studies office, and that this thesis has not been submitted for a higher degree to any other University or Institution.

Abstract

The Macdonald research group has long been interested in the synthesis of compounds containing low-valent main group elements. Recently, more work was put forth in the synthesis and study of molecules containing phosphorous in its +1 oxidation state (P^I).

One way of stabilizing the P^I center is by using *N*-heterocyclic carbenes (NHCs). Our group previously reported several approaches to salts containing $[(^R\text{NHC}^{R'})_2P^I]^+$ cations, most notably through ligand replacement reactions from precursors such as $[(\text{dppe})P^I]^+$ that we had developed previously.

Various derivatives of cyclic $[(^R\text{Bis})P^I]$ and acyclic $[(^R\text{NHC}^{R'})_2P^I]^+$ compounds have been synthesized. Experimental and computational investigation of the structural features, physical properties and reactivity patterns of such species are discussed. Evidence of π -delocalization from the electron rich phosphorus into the π -system is detailed with the cyclic system giving better delocalization due to the more planar arrangement forced by the bridging methylene. Oxidation and metal coordination reactions are performed on such compounds.

To my loving parents, Fouad & Suhaila!

Acknowledgements

I would like to start off by thanking my supervisor Dr. Chuck Macdonald for the opportunity and support he provided throughout my master's. Despite his busy schedule, Chuck always came out of his way to assist in guiding me to the right path; always providing prompt responses and feedback when questions arose. I would also like to thank Chuck for the motivation and help throughout the long PhD application process.

I would like to thank the Macdonald Group members, especially Greg Farrar, Raj Bandyopadhyay and Chris Allan for helping me getting started in the lab. I thank Jenn and Steph for the various conversations and hangouts we had. I also would like to thank the Johnson group members for all the fun in the office.

I would like to thank my undergraduate supervisor and current committee member, Dr. Eichhorn, for being such a great help throughout my undergraduate and graduate career here at the University of Windsor. I thank Dr. Rawson for all his help and for agreeing to be one of my graduate school referees. I would also like to thank Dr. Kedzierski for agreeing to be my Outside Departmental reader. Special thanks to Dr. Sam Johnson for being a great source of help in quadrupolar NMR and to Dr. Jim Green for all the organic chemistry help.

I thank my parents and my siblings for all the support, especially my mother for being a great example of a dedicated, hardworking individual. I thank her for being my inspiration and for always being there when needed. I could not have done it without her! A special thanks to Riham Aqel for encouragement and support.

Table of Contents

Declaration of Originality	iii
Abstract.....	iv
Dedication	v
Acknowledgements	vi
List of Tables	ix
List of Figures.....	x
List of Schemes	xi
List of Abbreviations/Symbols.....	xiii
1. Chapter 1 – Introduction	1
1.1. General Introduction	1
1.2. Oxidation States	2
1.3. Low Oxidation State Phosphorus Stabilization by Phosphines.....	7
1.4. Carbenes	12
1.5. Low Oxidation State Phosphorus Stabilization by <i>N</i>-Heterocyclic Carbenes	20
1.6. Using <i>N</i>-Heterocyclic Carbenes in the Activation and Stabilization of P₄	24
1.7. Dissertation Overview	28
2. Chapter 2 – Acyclic Phosphorus (+1) Stabilization by <i>N</i>-Heterocyclic Carbenes.....	29
2.1. Introduction.....	29
2.2. Experimental	31
2.3. Results and Discussions	39
2.3.1. Synthesis.....	39
2.3.2. NMR Analysis.....	43
2.3.3. Mass Spec Analysis	49

2.3.4. Computational Studies.....	51
2.4. Conclusions.....	59
3. Chapter 3 – Phosphorus (+1) Stabilization by Cyclic <i>N</i> -Heterocyclic Carbenes	60
3.1. Introduction.....	60
3.2. Experimental	62
3.3. Results and Discussions	68
3.3.1. Synthesis.....	68
3.3.2. NMR Analysis.....	71
3.3.3. Mass Spec Analysis	75
3.3.4. Computational Studies.....	77
4. Conclusions and Future Work	84
4.1. Conclusions.....	84
4.2. Future Work.....	86
5. References.....	88
Vita Auctoris.....	91

List of Tables

Table 2.1: Summary of crystallographic data for compounds 1 , 4 and 9	41
Table 2.2: Metrical parameters of the crystal structures 1 , 4 and 9	42
Table 2.3: Structures and ^{31}P NMR data of acyclic $(^{\text{R}}\text{NHC}^{\text{R'}})_2\text{P}^{\text{I}}$ compounds.....	43-44
Table 2.4: Calculated and found Mass Spec values for 6 , 7 and 8	50
Table 2.5: Bond distances and angles. DFT (PBE1PBE/TZVP)	51
Table 2.6: Energy gap calculations. DFT (PBE1PBE/TZVP)	53
Table 2.7: NBO WBI values for the model complexes. DFT (PBE1PBE/TZVP)	55
Table 2.8: Lone pair population and interaction. DFT (PBE1PBE/TZVP)	56
Table 2.9: TD calculation. TD-DFT (PBE1PBE/TZVP)	58
Table 3.1: Structures and ^{31}P NMR data of cyclic $[(^{\text{R}}\text{Bis})\text{P}^{\text{I}}][\text{Br}]$ salts and their oxidized variants.....	71
Table 3.2: Calculated and found Mass Spec values for 11-16 . DFT (PBE1PBE/TZVP)	76
Table 3.3: Bond distances and angles. DFT (PBE1PBE/TZVP)	77
Table 3.4: Energy gap calculations. DFT (PBE1PBE/TZVP)	79
Table 3.5: NBO WBI values for the model complexes. DFT (PBE1PBE/TZVP)	80
Table 3.6: Lone pair population and interaction. DFT (PBE1PBE/TZVP)	81
Table 3.7: TD calculations. TD-DFT (PBE1PBE/TZVP)	82

List of Figures

Figure 1.1: Inconsistencies between oxidation number and valence state in describing the oxidation state on the phosphorus center.....	4
Figure 1.2: Some examples that correlate Lewis structure to oxidation state based on the number of non-bonding electrons in the phosphorus center.....	5
Figure 1.3: Examples showing the ambiguity in non-bonding electron count in the various oxidation states of the central phosphorus in $[P(PR_3)_2]^+$	6
Figure 1.4: Illustration of different electronic configurations of carbenes.....	12
Figure 1.5: Illustration of the difference in bonding between (a) Fischer carbenes showing donor-acceptor bonding and (b) Schrock carbenes showing covalent bonding..	14
Figure 1.6: Examples of dicarbenes stable at room temperature.....	19
Figure 1.7: Di-coordinate phosphorus with P–C bond distance of: 1.756 – 1.760 Å.....	20
Figure 1.8: Illustration of σ and π orbitals of <i>N</i> -heterocyclic carbene and phosphine....	21
Figure 1.9: NHC-stabilized P(0) complex: NHC(P ₁₂)NHC.....	24
Figure 1.10: Robinson’s carbene stabilized di-phosphorus (P ₂).....	26
Figure 2.1: Thermal ellipsoid plots of the molecular structures of compounds 1 , 4 , 9 and 10	40
Figure 2.2: Labeling of protons and carbons in 1 and 9	45
Figure 2.3: Mass Spectra of 6 , 7 and 8 (Electrospray ionization).....	49
Figure 2.4: Geometry-optimized structures for model compounds 1' , 4'-10'	52
Figure 3.1: 1,1'-dibenzyl-3,3'-methylenediimidazole-2,2'-diylidene.....	61
Figure 3.2: Labeling of protons and carbons.....	72
Figure 3.3: Mass Spectra of 11-16 (Electrospray ionization).....	75
Figure 3.4: Geometry-optimized structures for model compounds 11'-16'	78

List of Schemes

Scheme 1.1: Reaction scheme of cyclic triphosphenium salt by Schmidpeter.....	8
Scheme 1.2: Reaction scheme of an acyclic triphosphenium salt.....	8
Scheme 1.3: Direct reduction of PI_3 to produce cyclic triphosphenium ion.....	10
Scheme 1.4: Synthesis of triphosphenium bromide.....	11
Scheme 1.5: An example of coordinating P^{I} to a transition metal, in this case, an acyclic triphosphenium ion is reacted with Schwartz Reagent.....	11
Scheme 1.6: Wanzlick's isolated NHC-metal complex.....	15
Scheme 1.7: Arduengo's synthesis of first stable <i>N</i> -heterocyclic carbene.....	16
Scheme 1.8: Kuhn's Carbene synthesis.....	17
Scheme 1.9: Hermann's synthesis of the free dicarbene.....	17
Scheme 1.10: Preparation of 1,1'-(pyridine-2,6-diyl)bis(3-benzyl-2,3-dihydro-1 <i>H</i> -imidazol-2-ylidene).....	18
Scheme 1.11: Dimroth's phosphamethine cyanine synthesis.....	21
Scheme 1.12: Schmidpeter's route to synthesizing P–C di-coordinate compounds.....	22
Scheme 1.13: Macdonald's direct synthesis of $[(^{\text{R}}\text{NHC}^{\text{R}})_2\text{P}^{\text{I}}][\text{Cl}]$ from PCl_3 and NHC..	22
Scheme 1.14: Macdonald's alternative approach to the synthesis of $[(^{\text{R}}\text{NHC}^{\text{R}})_2\text{P}^{\text{I}}][\text{Br}]$ using triphosphenium salt and NHCs.....	23
Scheme 1.15: Activation of P_4 using CAAC and NHC respectively.....	25
Scheme 1.16: Synthesis of $\text{Li}[\text{cyclo}-(\text{P}_5^{\text{f}}\text{Bu}_4)]$	27
Scheme 2.1: Schmidpeter's route to synthesizing P–C di-coordinate compounds.....	29
Scheme 2.2: Synthesis of $[(^{\text{Me}}\text{NHC}^{\text{Me}})_2\text{P}^{\text{I}}][\text{Br}]$	39
Scheme 2.3: Synthesis of $[(^{\text{Me}}\text{NHC}^{\text{Me}})_2\text{P}^{\text{I}}\text{H}][\text{Br}]$	46
Scheme 2.4: Synthesis of $[(^{\text{Me}}\text{NHC}^{\text{Me}})_2\text{P}^{\text{I}}\text{CH}_3][\text{Br}]$	46
Scheme 2.5: Synthesis of $[(^{\text{Me}}\text{NHC}^{\text{Me}})_2\text{P}^{\text{V}}\text{S}_2][\text{Br}]$	48

Scheme 2.6: Synthesis of $[(^{\text{Me}}\text{NHC}^{\text{Me}})_2\text{P}^{\text{I}}\text{AuCl}][\text{Br}]$ and $[(^{\text{Me}}\text{NHC}^{\text{Me}})_2\text{P}^{\text{I}}(\text{AuCl})_2][\text{Br}]$...	48
Scheme 3.1: synthesis of $[\text{Biscarbene-P}^{\text{I}}][\text{Br}]$ and its subsequent oxidation with sulfur.....	70
Scheme 4.1: Reacting $[(^{\text{Me}}\text{NHC}^{\text{Me}})_2\text{P}^{\text{I}}][\text{Br}]$ with a disulfide.....	86
Scheme 4.2: Reacting $[(^{\text{R}}\text{Bis})\text{P}^{\text{I}}][\text{Br}]$ with an equivalence of base to give the neutral overall compound shown with a connecting CH^- fragment.....	87

List of Abbreviations/Symbols

Å	Angstrom
Anal. Calc.	Analytically Calculated
Ar	Aryl
n-Bu	n-Butyl, (CH ₂) ₃ CH ₃
ⁿ BuBis	1,1'-di-n-butyl-3,3'-methylenediimidazole-2,2'-diylidene
Bz	Benzyl, (CH ₂)C ₆ H ₅
^{Bz} Bis	1,1'-dibenzyl-3,3'-methylenediimidazole-2,2'-diylidene
CAAC	Cyclic alkyl amino carbenes
CSD	Cambridge Structural Database
Cp	Cyclopentadienyl, C ₅ H ₅ ⁻
δ	Chemical Shift (NMR)
d	Doublet (NMR)
DCM	Dichloromethane
DFT	Density functional theory
DMSO	Dimethylsulfoxide
dec.	Decomposition
dppe	1,2-bis(diphenylphosphino)ethane, Ph ₂ P(CH ₂) ₂ PPh ₂
dppp	1,3-bis(diphenylphosphino)propane, Ph ₂ P(CH ₂) ₃ PPh ₂
dppb	1,2-bis(diphenylphosphino)butane, Ph ₂ P(CH ₂) ₄ PPh ₂
E	Element
EA	Elemental analysis
eq.	Equivalence
ERO	Electron-Rich Olefin
Et	Ethyl, CH ₂ CH ₃
^{Et} NHC ^{Me}	1,3-diethyl-4,5-dimethylimidazol-2-ylidene
HOMO	Highest unoccupied molecular orbital
HRMS-ES	High resolution mass spectrometry
Hz	Hertz
ⁱ Pr	Iso-propyl, CH(CH ₃) ₂
^{iPr} NHC ^{Me}	1,3-diisopropyl-4,5-dimethylimidazol-2-ylidene
IUPAC	International Union of Pure and Applied Chemistry
ⁿ J _{XY}	n-bond coupling constant between nuclei x and y
L	Neutral ligand
LUMO	Lowest unoccupied molecular orbital
M	Metal Atom
m	Multiplet (NMR)

Me	Methyl, CH ₃
^{Me} Bis	1,1'-dimethyl-3,3'-methylenediimidazole-2,2'-diylidene
^{Me} NHC ^{Me}	1,3,4,5-tetramethylimidazol-2-ylidene
MeOTf	Methyl trifluoromethanesulfonate (CF ₃ SO ₂ OCH ₃)
Mes	Mesityl, 2,4,6-trimethylphenyl, Me ₃ C ₆ H ₂
mmol	Millimole
Mp	Melting point
NBO	Natural bond order
NHC	N-heterocyclic carbene
NMR	Nuclear Magnetic Resonance
OTf	Triflate, SO ₃ CF ₃ ⁻ , trifluoromethanesulfonate
p	Pentet (NMR)
Ph	Phenyl, C ₆ H ₅
Pn	Pnictogen, Group 15 element: N, P, As, Sb, Bi
ppm	parts per million
q	Quartet (NMR)
R	Any organic substituent
s	Singlet (NMR)
t	Triplet (NMR)
^t Bu	tert-butyl, C(CH ₃) ₃
THF	Tetrahydrofuran
TMS	Trimethylsilyl, SiMe ₃
Triflate	Trifluoromethanesulfonate
WBI	Wiberg bond index
Triflic Acid	Trifluoromethanesulfonic acid (CF ₃ SO ₂ OH)
X	Halogen atom

1. Chapter 1 – Introduction

1.1. General Introduction

In the periodic table, groups are usually referred to by Arabic or Roman numerals.¹ Group 15 (in Arabic numerals) or VA (using the older convention with Roman numerals) consists of the elements: nitrogen, phosphorus, arsenic, antimony and bismuth.² This group is usually referred to as "pnictogens" (as well as "the nitrogen family"), which comes from the Greek word "pniktos" meaning to "choke or strangle". The term "pnictogens" will be denoted as "Pn" throughout this thesis in reference to Group 15 elements. In their elemental forms, the physical and chemical properties of these pnictogens vary considerably. Nitrogen is found as a non-metal diatomic gas, phosphorus has different allotropes but is a non-metal solid in most of these allotropes, arsenic and antimony are metalloids and bismuth is a metal.

Our research group has long been interested in the synthesis of compounds containing low-valent main group elements. The primary focus of this thesis is on the element phosphorus in the unusually low +1 oxidation state. The most common form of elemental phosphorus, phosphorus (0), is white (P_4); other common forms exist such as red and black phosphorus which consist of ill-defined polymeric structures. It should be noted that none of these forms occurs naturally on Earth and phosphorus compounds generally contain the element in the formal +3 or +5 oxidation state.

1.2. Oxidation States

Oxidation state is the concept of assigning a number to an atom that provides a hypothetical charge indicating the degree of oxidation (i.e. the number of electrons that have been formally removed from the neutral atom) and which would give an insight to the reactivity of the molecule in which the atom is present. The concept of assigning an oxidation state dates back to the late 18th century where it was introduced by French chemist, Antoine Lavoisier. It was at the time that oxidation and reduction were first used in literature in reference to reactions taking place between oxygen and other elements.³ Now, that we understand that chemistry is all about electrons and electrons play a major role in all chemical bonds. It is clear that a method to assign electrons to atoms may provide insight into its chemistry. These days, terms including valence state (VS) and oxidation number (ON) are used in literature to serve the purpose of assigning an oxidation state to an atom. These concepts are fundamental to the study of chemistry and are introduced to students as early as high-school. Other useful concepts such as formal charge and coordination number are sometimes confused with oxidation states. More importantly, it should be noted that the terms "oxidation number" (or "oxidation state") and "valence state" are often (and incorrectly) used interchangeably to describe the same thing so it is worth providing some clarification about the specific meaning of each term and an indication of how they will be used in this thesis.⁴

The assignment of an oxidation state to an atom is accomplished on the basis of oxidation number⁵ rules but the number can also be misleading because it does not take into consideration the actual distribution of electrons or the chemical behaviour of a compound. The most common method of counting is based on the difference in the

electronegativity of the atoms being accounted for. In this kind of assignment, there are a few axioms such as hydrogen is assigned +1 oxidation number and oxygen is assigned a -2 oxidation number. Aside from these two rules, usually the atom with higher electronegativity is assigned a negative charge while the atom with the lower electronegativity is assigned the positive charge. Pnictogens have a whole range of oxidation states based on these electron counting rules which span a range of -3 to +5.⁶ This system is imperfect and one example of the inconsistencies it holds is the comparison between Li_3P and PH_3 . They both have formal oxidation states of -3 although they have very different chemical properties. Another example of the inconsistencies is the comparison between PH_3 and AsH_3 where they have formal oxidation states of -3 and +3, respectively, in spite of their similar chemical, electronic and structural behaviour.

The other common method of oxidation state assignment is the concept of the valence state. The valence state is a measure of the number of electrons an atom uses for bonding (or charges). For example, in CH_4 , carbon has a valence of 4, meaning that all four electrons in the atom are used for making bonds (or charges) while hydrogen has a valence of 1, and uses its single electron for chemistry. In contrast to formal oxidation states, which can usually be derived on the basis of the molecular formula, one must know the actual arrangement of the electrons within the molecule to assign valence states. Because of this specificity, the valence state model is usually much more helpful in terms of understanding the chemical structure and reactivity of a molecule. Just as with the previous case, valence state assignment is imperfect and shows unintuitive description of

the oxidation state that would not be in agreement with the oxidation number as shown in

Figure 1.1; thus, we prefer to use a more convenient model.

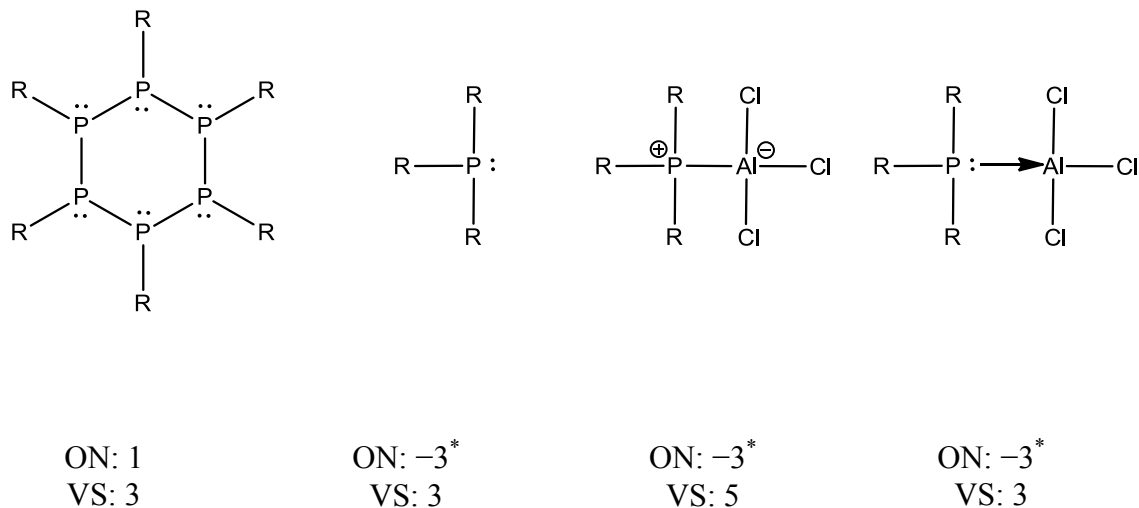


Figure 1.1: Inconsistencies between oxidation number and valence state in describing the oxidation state on the phosphorus center.

*The charge on phosphorus can be positive or negative depending on the R group. In this case, the R group is assumed to be less electronegative than phosphorus.

This more convenient model is used in the Macdonald group where the above inconsistencies are accounted for and would give a more justifiable oxidation state, thus, diminishing the ambiguity of using the previous two counting methods. The notation used in our group is as follows: phosphorus with no lone pairs is in the +5 oxidation state: P^V , phosphorus with one lone pair is in the +3 oxidation state: P^{III} , phosphorus with two lone pairs is in the +1 oxidation state: P^I , phosphorus with three lone pairs is in the -1 oxidation state: P^{-I} and phosphorus with four lone pairs is in the -3 oxidation state: P^{-III} . This method can be used for all pnictogens and any other atom. One can see that it's also possible to account for negative oxidation states using this model although such cases are

relatively rare for molecular species containing phosphorus. Overall this convention gives a better representation of the reactivity and bonding of a molecule while still giving an insight on the structure (i.e. accounting for the number of non-bonding electrons in an atom). **Figure 1.2** shows examples of the oxidation states of phosphorus based on this counting method. It is also worth noting that donor-acceptor bonds can also be used in this system (in which the electrons are still considered to be present on the donor) to avoid odd assignments such as the valence state of 5 for P in the phosphine-alane adduct in **Figure 1.1**.

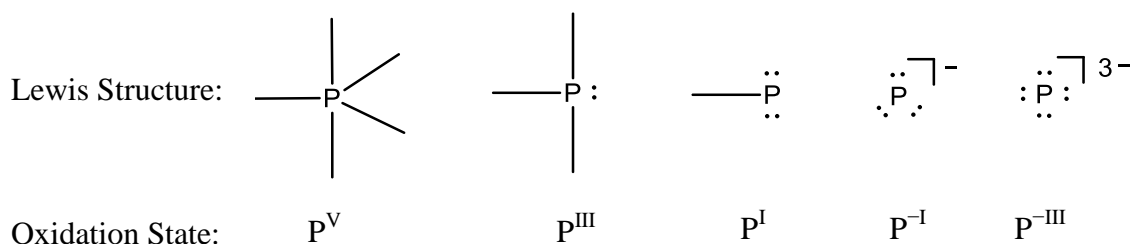


Figure 1.2: Some examples that correlate Lewis structure to oxidation state based on the number of non-bonding electrons in the phosphorus center.

One problem that is apparent with the valence state (and Macdonald) systems is solely due to the ambiguity that arises when drawing a Lewis structure such as the examples shown in **Figure 1.3**. It is true that the most likely structure or the most favourable one would be the one used in counting the unpaired electrons around the atom but one must remember that Lewis structures are a simple model that is used to illustrate the basic connectivity of a molecule in a way that includes all of the electrons present. In

reality, it requires more sophisticated methods to determine the actual number of unpaired electrons on an atom such as computation.⁶

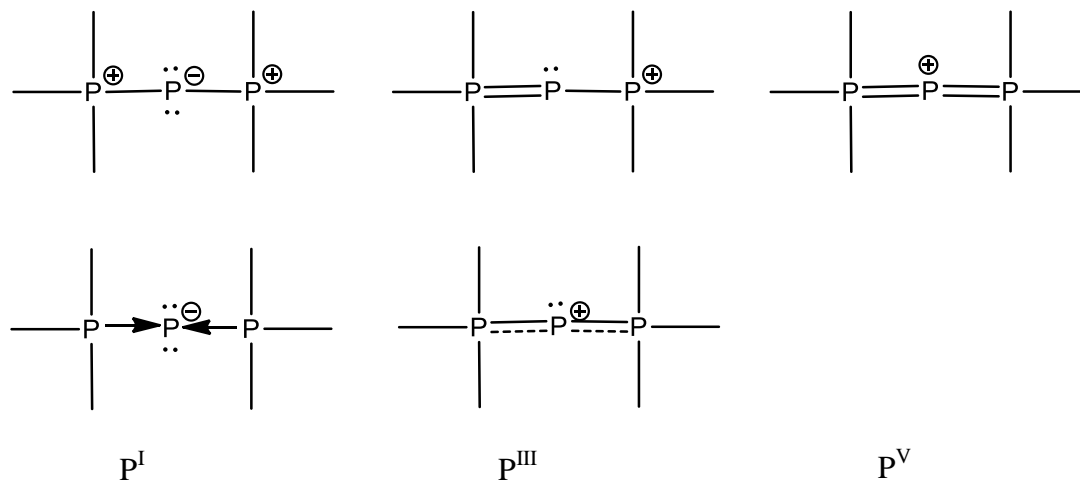


Figure 1.3: Examples showing the ambiguity in non-bonding electron count in the various oxidation states of the central phosphorus in $[P(PR_3)_2]^+$.

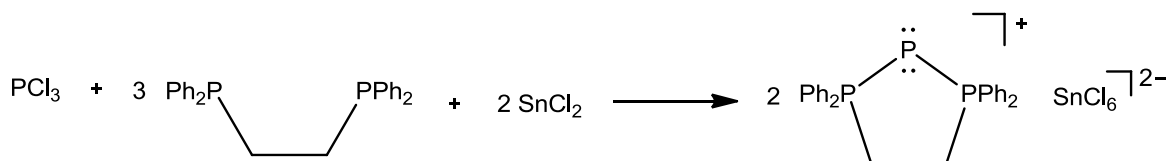
1.3. Low Oxidation State Phosphorus Stabilization by Phosphines

Ligands containing main group elements bearing "lone pairs" of electrons have been ubiquitous for the preparation of transition metal complexes. Interest in the synthesis and study of low oxidation main group elements has grown rapidly and the study of phosphorus in low oxidation states has been an active area of study for many years.⁶ One common class of stable compounds containing monovalent phosphorus is salts containing triphosphenium cation of the general formula $[\text{R}_3\text{P}-\text{P}-\text{PR}_3]^+$. The central dicoordinate phosphorus atom is electron rich phosphorus in the +1 oxidation state which results in different structural features and reactivity properties as compared to +3 and +5 oxidation state analogues.

As illustrated in **Figure 1.3**, there are several possible structures that one might predict for the cationic fragment $[\text{R}_3\text{P}-\text{Pn}-\text{PR}_3]^+$. If the compound contains a Pn^{V} center, one would expect the geometry to be linear. This linear arrangement is found for compounds like bisphosphoranyliminim salts with the general formula $\text{P}-\text{N}-\text{P}$, which contain N^{V} atoms. This kind of arrangement is not observed for heavier pnictogen analogues such as triphosphenium cations: $[\text{R}_3\text{P}-\text{P}-\text{PR}_3]^+$. Instead, the structural features of all observed triphosphenium cations suggest that P^{I} or P^{III} descriptions are more appropriate: each of which would contain a bent structure with bond distances shorter than those of a single P–P bond due to delocalized π -bonding or Coulombic attraction.⁶

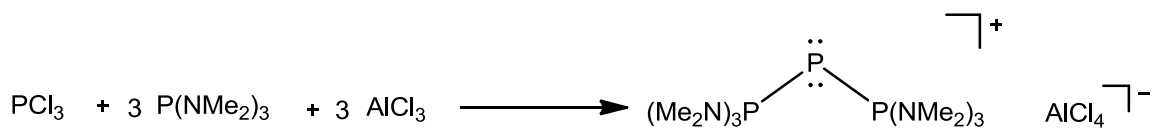
Cyclic triphosphenium ions were first synthesized and characterized by X-ray crystallography in 1982 by Schmidpeter and coworkers.⁷ This triphosphenium salt was

synthesized by the reduction of PCl_3 with SnCl_2 in the presence of 1,2-bis(diphenylphosphino)ethane or dppe (**Scheme 1.1**).



Scheme 1.1: Reaction scheme of cyclic triphosphenium salt by Schmidpeter.

This general scheme was used to synthesize different cyclic and acyclic triphosphenium cations using different reducing agents.⁸⁻¹⁰ The acyclic systems are less thermally stable than the cyclic ones; however, a reaction like the one shown in **Scheme 1.2** generates a thermally stable acyclic triphosphenium center.¹⁰

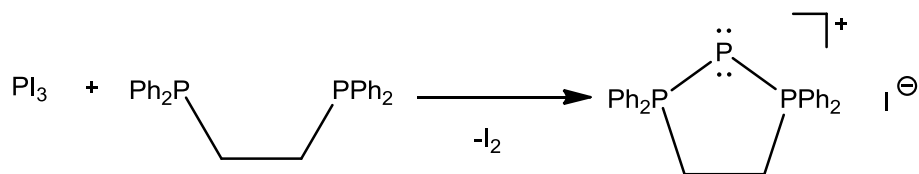


Scheme 1.2: Reaction scheme of an acyclic triphosphenium salt.

Different groups have worked on improving the synthesis of triphosphenium salts by developing reaction pathways that do not involve the use of external reducing agents. Dillon's¹¹⁻¹⁴ group in 2001 reached this mile stone and was followed by the Macdonald¹⁵⁻¹⁷ group.

Dillon's group has shown that the reaction of PX_3 ($X = Cl, Br$ or I) with dppe formed a five membered ring readily in DCM. NMR data with distinctive triplet and doublet patterns confirmed the identity of this cyclic triphosphenium ion which are in close agreement with the results of Schmidpeter. Other cyclic triphosphenium ions were also synthesized that include dppp (1,2-bis(diphenylphosphino)pentane) and dppb (1,2-bis(diphenylphosphino)butane) which form 6 and 7 membered rings respectively.¹¹ The general synthetic scheme followed is the direct reduction of PX_3 using diphosphine to produce the triphosphenium salt. Diphosphine also reacts with the X_2 that is formally produced during the reaction generating a halo-phosphonium salt as a by-product; unfortunately, the presence of this by-product meant that none of the triphosphenium salts produced in this manner could be isolated, purified or crystallized.¹¹ In 2001, Dillon's group further extended this library of compounds by synthesizing more triphosphenium salts and by synthesizing some arsenic analogues of these salts.¹² Further chemistry was performed a few years later which included methylation of the phosphorus center.¹³ With this kind of system, oxidation reactions such as alkylation and protonation have been performed and documented. Reagents such as methyl triflate and triflic acid are used to pursue such oxidation reactions to give a methylated and a protonated P^{III} center, respectively.^{13,14}

The synthesis of triphosphenium salts was further improved by Macdonald and coworkers where PI_3 is reacted in a similar manner with diphosphine to generate a cyclic triphosphenium ion and I_2 . The major improvement is that the eliminated I_2 is easily washed away with THF (**Scheme 1.3**) allowing for the isolation of pure, crystalline product for the first time:¹⁵

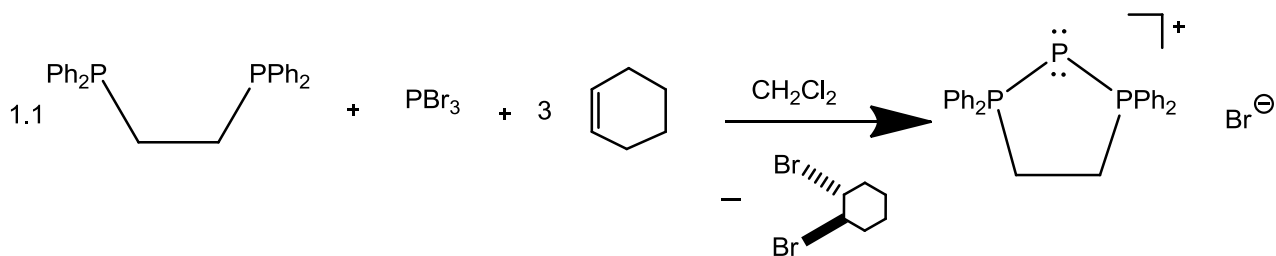


Scheme 1.3: Direct reduction of PI_3 to produce cyclic triphosphenium ion.

This reaction was also performed using PCl_3 and PBr_3 , but did not result in a pure triphosphenium salt ion. It is proposed that the Cl_2 and Br_2 produced by this process are too reactive (in comparison to I_2) and will readily oxidize the diphosphine ligand giving multiple side products that are observed in the ^{31}P NMR. The synthesized triphosphenium iodide is air stable and its remarkable stability is attributable to the presence of π -electron donation from the electron rich P^{I} center to the anti-bonding π^* orbitals of the dppe phosphorus.¹⁵ The Macdonald group also reported that the reaction of two equivalents of dppe with P_2I_4 produces the triphosphenium iodide.¹⁵ Following this work, Woollins group reported the synthesis of the triphosphenium iodide using of P_2I_4 and 1,8-bis(diphenylphosphino)naphthalene.¹⁸ The reason why triphosphenium iodide is an important source of P^{I} ion is the fact that with iodine, it would be possible to access a whole variety of different anions through simple metathesis reactions which are useful to access further chemistry with these P^{I} fragments.

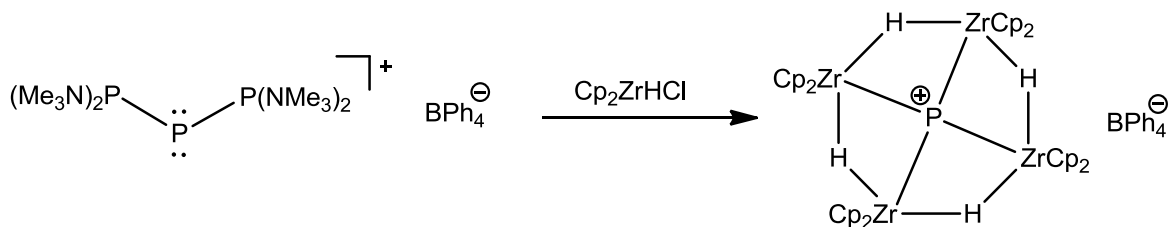
The synthesis of triphosphenium bromide came in 2008 by the work of Norton from the Macdonald group in which the new synthetic pathway created an even cleaner approach to obtaining the triphosphenium ion. The isolated yield obtained from triphosphenium iodide was 52% while triphosphenium bromide synthesis gave a yield of

as high as 96%. The synthesis proceeds as follows: an equivalent of PBr_3 and three equivalents of cyclohexene are added to a slight excess dppe in dichloromethane under inert conditions. The produced bromine (Br_2) is sequestered by cyclohexene to produce (S,S) (or (R,R)) 1,2-dibromocyclohexane which is easily removed under vacuum (**Scheme 1.4**).¹⁷



Scheme 1.4: Synthesis of triphosphenium bromide.

Methylation and protonation are not the only oxidation reactions that can be done with these triphosphenium salts. An interesting oxidation reaction that can be done with the P^{I} center is the coordination of P^{I} to a transition metal center. An example of this is the work reported by Driess where an acyclic triphosphenium ion was reacted with excess Schwartz Reagent $[(\text{Cp})_2\text{ZrHCl}]$ to yield a planar tetracoordinate phosphorus center as depicted in **Scheme 1.5**.¹⁹



Scheme 1.5: An example of coordinating P^{I} to a transition metal, in this case, an acyclic triphosphenium ion is reacted with Schwartz Reagent.

1.4. Carbenes

Carbenes have played an important role in transient intermediates where it was introduced into the organic world in the 1950s and the organometallic world in 1964 after the work of Fischer. A carbene is a neutral molecule that has a two coordinate, divalent carbon with 6 valence electrons around the carbene carbon center. The carbene carbon assumes a linear or bent geometry depending on the hybridization on that carbon center, where a linear arrangement suggests an sp hybrid orbital and a bent arrangement suggests an sp^2 hybrid orbital. The non-bonding electrons can be either paired (singlet) or unpaired (triplet). These singlet and triplet states are illustrated in **Figure 1.4**.²⁰

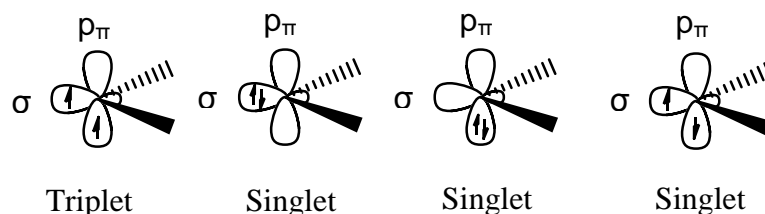


Figure 1.4: Illustration of different electronic configurations of carbenes.

As depicted in the figure above, the first case is a triplet state ($\sigma^1 p_\pi^1$) in which electrons are in different orbitals with parallel spins. The second case is a σ^2 singlet state where electrons are in the sigma orbital and are of opposite spins. The configuration is a p_π^2 singlet state of electrons in the p orbital with opposite spins. The last configuration is a $\sigma^1 p_\pi^1$ excited singlet state in which electrons are of opposite spins and are in different orbitals. The multiplicity of the ground-state spin is important in determining the reactivity of the carbene. Substituents on the carbene would influence the ground-state multiplicity and thus the reactivity of the carbene which would best be analyzed by

looking at the electronic and steric effects of these substituents. Studying the synthetic approach and kinetics of carbenes are also important.²⁰

Electronic effects can be divided into inductive and mesomeric effects. For the inductive effect, it is well established that substituents that are σ electron withdrawing would favour having a singlet state over a triplet state. This is the case because σ non-bonding orbitals are stabilized by the increased s character which increases the gap between σ and p_π favouring singlet state. On the other hand, having a σ donor substituent will decrease the gap between σ and p_π , as σ is destabilized which will favour the triplet state.^{20,21}

It is true that inductive effects play a role in the ground-state multiplicity, but mesomeric effects play an even bigger role in dictating the multiplicity of a carbene. π -donor substituents donate electron density into the empty p_π orbital making a four-electron three-center π -system. One factor that helps in stabilizing the carbene is the fact that most of these substituents have greater electronegativity than carbon allowing the carbon to act as a σ -acceptor which in turn, stabilizes the carbene lone pair. Bulky substituents stabilize carbenes and they can influence to the ground-state spin multiplicity if the electronic effects are negligible.

Increasing steric bulk of substituents will cause bending in the carbene bond favouring the triplet state and thus, using bulky groups has been the way to stabilize triplet state carbenes. This increase in the p_π character comes from decreased carbene bond angle or increased carbene bond lengths.^{20,22}

Carbenes have played an important role in organometallic chemistry wherein carbenes have been used to form metal carbon bonds. Fischer and Schrock carbenes have both been used for this purpose and carbene coordination has been reported to almost all transition metals. The metal carbon bond formed from coordinating Fischer carbenes to transition metals is a donor-acceptor bond which allows for superpositioning of the carbene by metal-carbon σ -donation and carbene-metal π -back-donation.^{20,23} Schrock carbenes on the other hand form complexes that are more covalently bonded and that usually results from the interaction of the triplet state of the carbene with the triplet state of the metal center. Fischer carbenes interact with low-valent metals while Schrock carbenes interact with high oxidation state metals. Schrock carbenes are usually alkyl substituted while Fischer carbenes have substituents that possess π -donation ability. The difference in bonding between the two carbenes is illustrated in **Figure 1.5**.²⁰

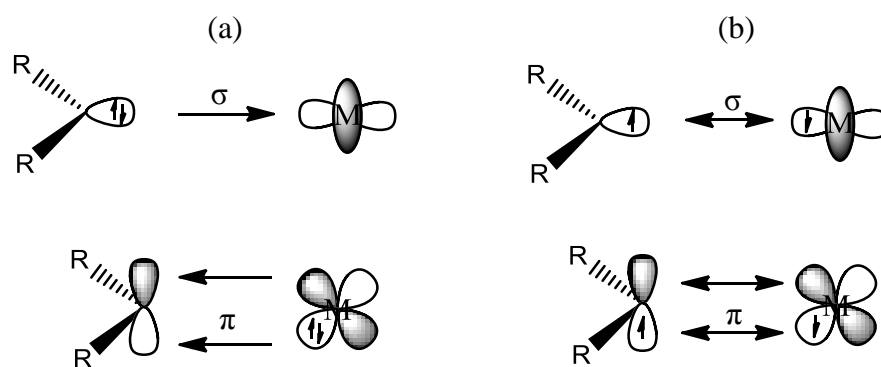
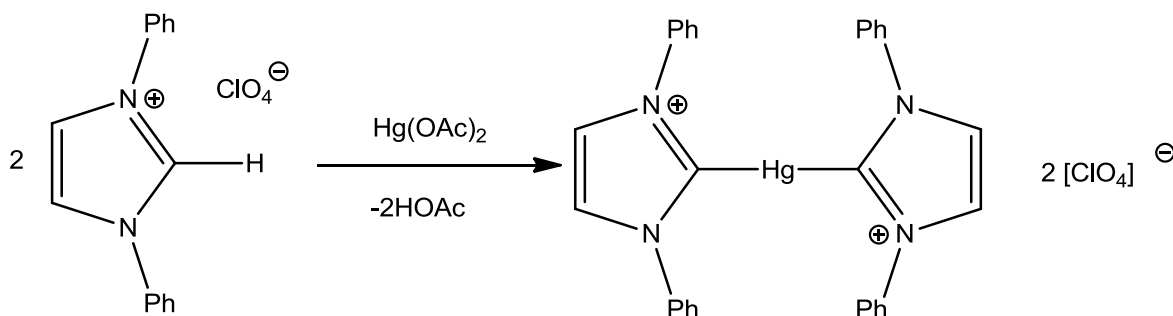


Figure 1.5: Illustration of the difference in bonding between (a) Fischer carbenes showing donor-acceptor bonding and (b) Schrock carbenes showing covalent bonding.

Another class of carbenes is the stable persistent carbenes or sometimes known as Arduengo carbenes among which *N*-heterocyclic carbenes (NHCs) belong.²⁴ NHCs are

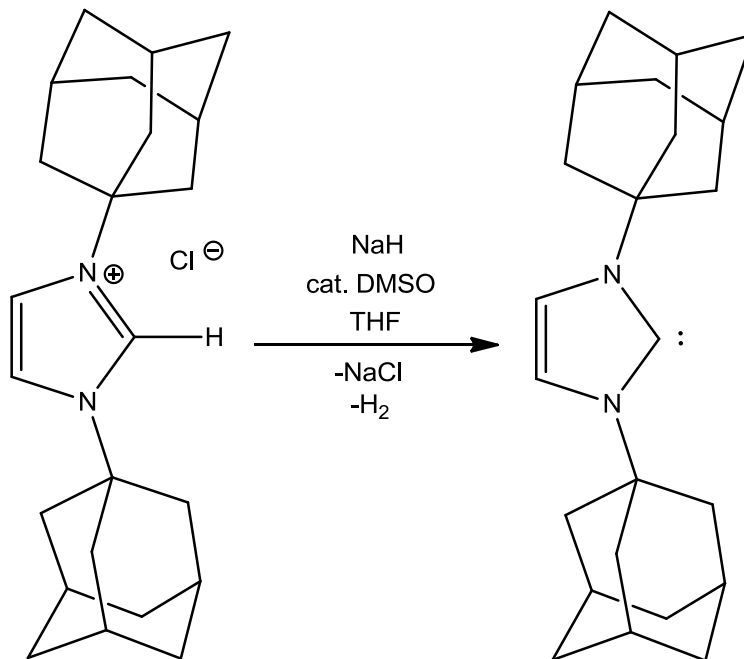
the most common class of carbenes among these persistent carbenes. These *N*-heterocyclic carbenes are diaminocarbenes with the general formula of $(R_2N)_2C:$. The work of Wanzlick presented the first examples of NHCs²⁵ and in 1970, Wanzlick and co-workers showed that imidazolium salts can be deprotonated by potassium *tert*-butoxide to give imidazol-2-ylidenes which were synthesized but not isolated. It was trapped by using a metal complex to simultaneously coordinate and stabilize the carbene as generated. This was achieved by reacting diphenyl imidazolium salt with mercury (II) acetate. In this case, the acetate acted as the base to deprotonate the imidazolium salt and the carbene generated coordinated to mercury as shown in **Scheme 1.6**.²⁶ It was not until 20 years later that Arduengo *et al.* prepared and isolated stable carbene compounds.²⁴



Scheme 1.6: Wanzlick's isolated NHC-metal complex.

Thus, after a long period of time, Arduengo's work was a driving force to re-initiate interest in synthesizing stable, collectable and storable carbenes. The first synthesized *N*-heterocyclic carbene to be collected and characterized was 1,3-di-1-adamantylimidazol-2-ylidene. This NHC was synthesized by using the same idea first proposed by Wanzlick with minor changes to the reaction protocol. The difference is that

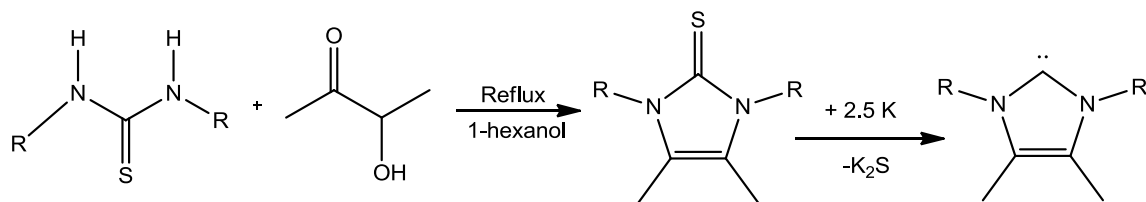
base like NaH was used along with a catalyst (DMSO) to deprotonate the imidazolium salt. The reaction is outlined in **Scheme 1.7**.



Scheme 1.7: Arduengo's synthesis of first stable *N*-heterocyclic carbene.

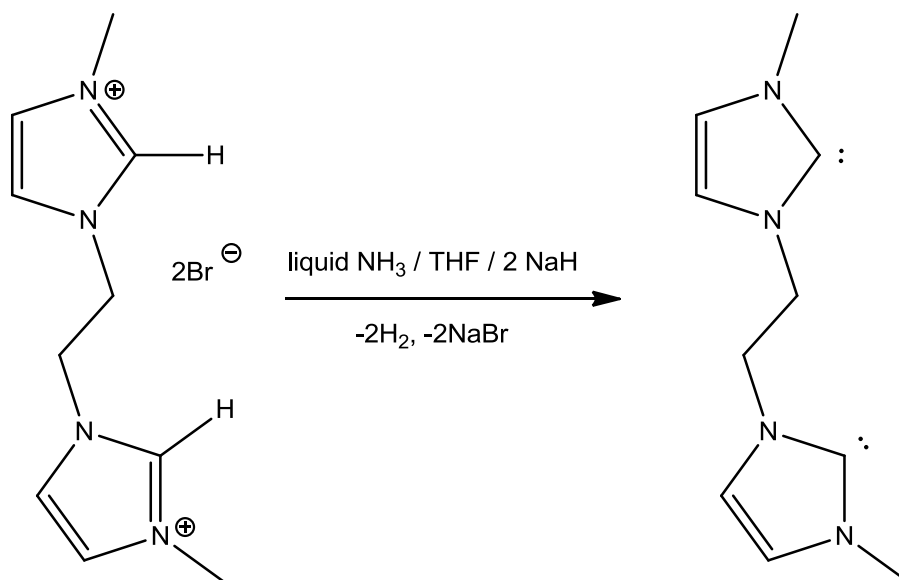
Initially, it was hypothesized that the stability of Arduengo carbenes is derived from a combination of steric and electronic effects, but in 1992, Arduengo *et al.* were successful in preparing several more stable carbenes in which the structural features of these new carbenes suggested that steric factors do not play an important role in their stability.²²

Other approaches to carbenes have been reported, one of which is the work of Kuhn in 1993. Kuhn's syntheses involves desulfurization of imidazolin-2-thiones to obtain the corresponding imidazol-2-ylidene as shown in **Scheme 1.8**.²⁷



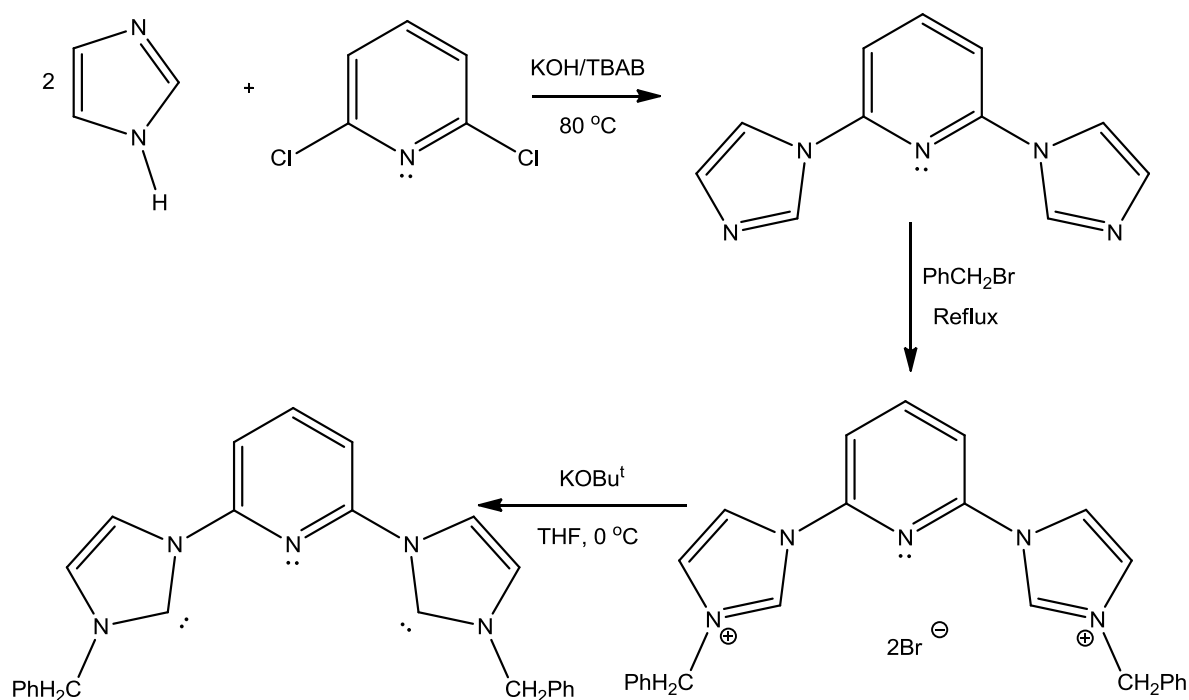
Scheme 1.8: Kuhn's Carbene synthesis.

A vast library of different carbenes has been synthesized since then and one interesting class of these *N*-heterocyclic carbenes is the linked NHCs or dicarbenes, where two imidazol-2-ylidenes are bridged together by a backbone linker. This linker can be a CR_2 , BR_2 or even a transition metal fragment. Synthesis of dicarbenes was introduced late in literature compared to the time free NHC was first reported. The isolation of liquid dicarbenes was first reported in 1989 by Bertrand *et al.*²⁸ In 1996, Hermann and co-workers developed a new method in deprotonating imidazolium salts which involved the use of metal amides such as sodium amide in the presence of liquid ammonia in THF to give a variety of stable carbenes and dicarbenes.^{29,30} (**Scheme 1.9**)



Scheme 1.9: Hermann's synthesis of the free dicarbene.

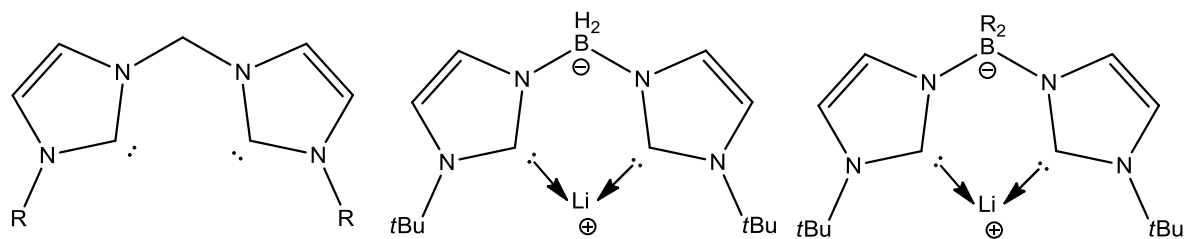
After the work of Herrmann, other synthetic approaches have been developed towards the synthesis of stable dicarbenes. One example is the pyridine-containing dicarbenes as illustrated in **Scheme 1.10**.^{31,32}



Scheme 1.10: Preparation of 1,1'-(pyridine-2,6-diyl)bis(3-benzyl-2,3-dihydro-1*H*-imidazol-2-ylidene)

One problem with this class of dicarbenes is their extreme sensitivity to temperature and moisture. Leaving the free dicarbene at room temperature will degrade the carbene even if it was in solution for a short period of time under inert conditions and thus, usually NMR data of these dicarbenes are collected soon after mixing while the solution is still at low temperatures. Also, any further coordination chemistry done is usually done *in situ*.^{30,32} Only recently, some groups were successful at synthesizing

dicarbenes that are isolated and are stable at room temperature.³³⁻³⁵ Examples of these are shown in **Figure 1.6**.



R= benzyl or p-^tButylBenzyl

R= phenyl or methyl

Figure 1.6: Examples of dicarbenes stable at room temperature.

1.5. Low Oxidation State Phosphorus Stabilization by *N*-Heterocyclic Carbenes

An important land mark in the history of phosphorus chemistry is the synthesis of di-coordinate phosphorus compounds that were crystallographically-characterized. An example of this class of compounds is illustrated in **Figure 1.7** which showed proof of P–C multiple bonding. The synthetic route to get to this di-coordinate phosphorus was a problem due to the fact that the synthesis involved explosive or pyrophoric reagents such as $\text{P}(\text{CH}_2\text{OH})_3$ or $\text{P}(\text{SiMe}_3)_3$ respectively and thus this initiated interest in developing safer routes to synthesizing such structures.³⁶⁻³⁸

Compounds of the form $\text{P}=\text{R}$ bonds are known as phosphinidenes and they make up the largest class of compounds containing phosphorus in its +1 oxidation state. This specific class of phosphinidenes is known as phosphamethine cyanine which is important in main group chemistry due to the fact that they were the first structures synthesized and isolated that contained P–C π -bonding. Cyanines are synthetic dyes containing a conjugated chain that usually contain heterocyclic systems such as imidazole, pyridine, pyrrole and others.⁵ It is not only important for that fact alone, but because it is also the first group of compounds that were isolated with carbon involved in π -bonding with a main group element beyond period II.³⁹

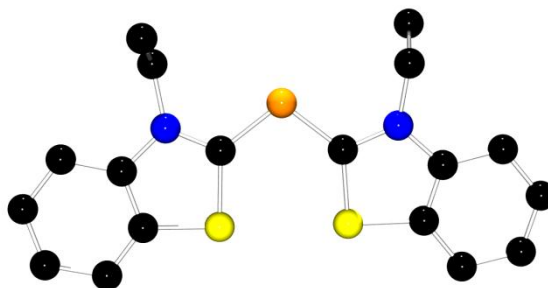
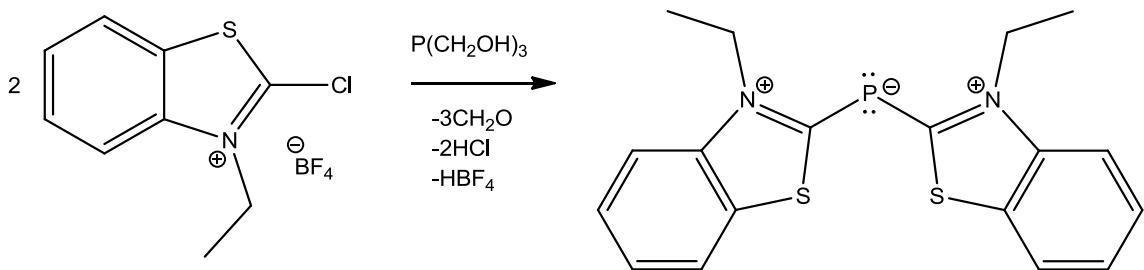


Figure 1.7: Di-coordinate phosphorus with P–C bond distance of: 1.756 – 1.760 Å

The work by Dimroth in 1964 led to the synthesis of phosphamethine cyanines where tris(hydroxymethyl)phosphane or tris(trimethylsilyl)phosphines were mixed with a haloimidazolium salt to give the desired di-coordinate phosphorus as illustrated in **Scheme 1.11**.³⁶



Scheme 1.11: Dimroth's phosphamethine cyanine synthesis.

Phosphines and *N*-heterocyclic carbenes are very comparable and their similarities have been discussed by Bertrand.²⁰ The electronic similarities between the two were first discussed by Hermann. As illustrated in **Figure 1.8**, both ligands coordinate through σ -donation to a metal center. Both have π -accepting ability, but π -back donation is very weak in *N*-heterocyclic carbenes due to the fact that the empty p_π orbitals are very high in energy when compared to p_π orbitals in phosphines. Although NHCs have weaker π -back donation ability, but they have much better σ bonds and possesses stronger σ -donation ability than phosphines.⁴⁰

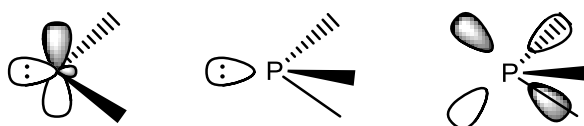
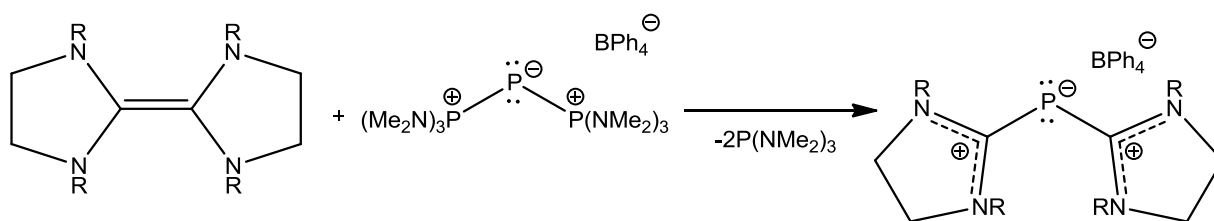


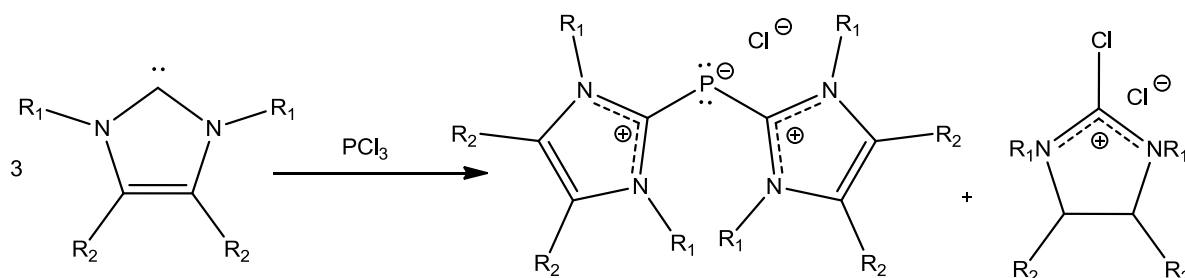
Figure 1.8: Illustration of σ and π orbitals of *N*-heterocyclic carbene and phosphine.

After the work of Dimroth, Schmidpeter *et al.* reported reacting triphosphenium salt $\text{P}[\text{P}(\text{NMe}_2)_3]_2[\text{BPh}_4]$ with a carbene dimer to give a di-coordinate phosphorus as illustrated in **Scheme 1.12**.⁴¹ This approach of synthesizing P–C di-coordinate fragments represents a safer route of synthesis than the one reported by Dimroth which involved explosive and pyrophoric reagents.



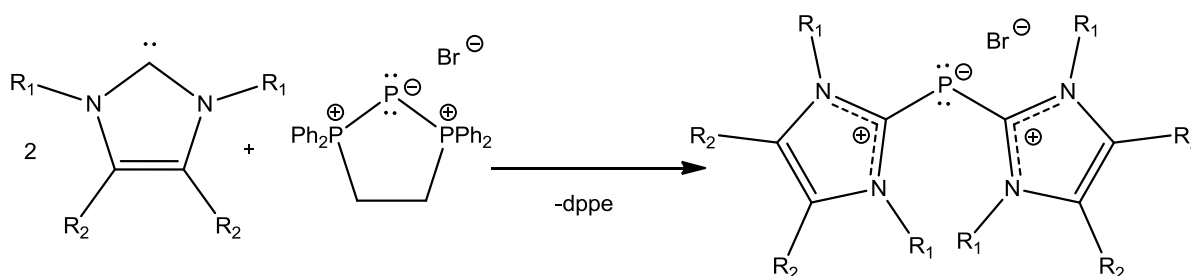
Scheme 1.12: Schmidpeter's route to synthesizing P–C di-coordinate compounds.

Since Arduengo's report of stable *N*-heterocyclic carbenes in 1991, NHCs have been used in different fields, one of which is coordination chemistry. The Macdonald group in 2005 investigated carbene-stabilized P^{I} cations and has since developed synthetic methods to obtain NHC-stabilized P^{I} cations.⁴² Following the protocols used for triphosphenium synthesis, the reaction of PCl_3 with three equivalents of NHC produces the expected $[(^{\text{R}}\text{NHC}^{\text{R}'})_2\text{P}^{\text{I}}][\text{Cl}]$ and the other equivalent of NHC is used up in the reaction with the Cl_2 by-product. The reaction is outlined in **Scheme 1.13**.



Scheme 1.13: Macdonald's direct synthesis of $[(^{\text{R}}\text{NHC}^{\text{R}'})_2\text{P}^{\text{I}}][\text{Cl}]$ from PCl_3 and NHC

This synthetic route gave the product, but the presence of the chloroimidazolium chloride by-product made it hard to isolate the $[(^R\text{NHC}^{R'})_2\text{P}^I][\text{Cl}]$ product due to the similar solubilities the product and by-product share. Another approach to getting this P^I product cleanly is using triphosphenium salts as a precursor along with two equivalents of NHC. This reaction produces P^I salts containing $[(^R\text{NHC}^{R'})_2\text{P}^I]^+$ cations through a ligand replacement mechanism in which the weaker phosphine ligand is displaced by the stronger NHC donor. This reaction is illustrated in **Scheme 1.14** and comparing this reaction to the previous method, it is worth noting that this reaction is much cleaner in the sense that the by-product (dppe) is easily washed away with non-polar solvents such as pentane or toluene giving the a pure product that is easily collected from non-polar solvents.⁴²



Scheme 1.14: Macdonald's alternative approach to the synthesis of $[(^R\text{NHC}^{R'})_2\text{P}^I][\text{Br}]$ using triphosphenium salt and NHCs

1.6. Using *N*-Heterocyclic Carbenes in the Activation and Stabilization of P₄

The activation of white phosphorus (P₄) is a topic of current interest and different groups seek a more sustainable route to the production of organophosphorus compounds. Usually, this can be achieved by the use of transition metals and main group elements. NHCs have been involved in the activation reactions of P₄ starting with the work of Bertrand *et al.* in 2007.^{43,44}

Activating P₄ with carbenes has provided a safer route to the activation of white phosphorus than previous routes. For example, the treatment of P₄ with NHC produces phosphorus with a formal zero oxidation state. An example is NHC(P₁₂)NHC as shown in **Figure 1.9**.⁴⁴ The ³¹P NMR spectra shows 10 signals in the intensity ratio of 1:1:1:1:1:1:1:1:3:1 which suggests a P₁₂ cluster of which the structure has been characterized by single crystal X-ray diffraction.

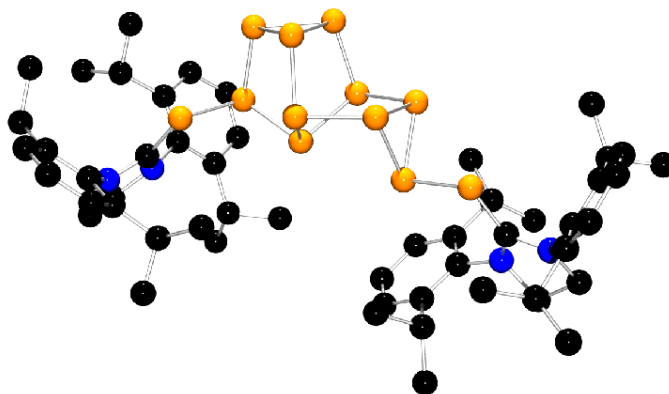
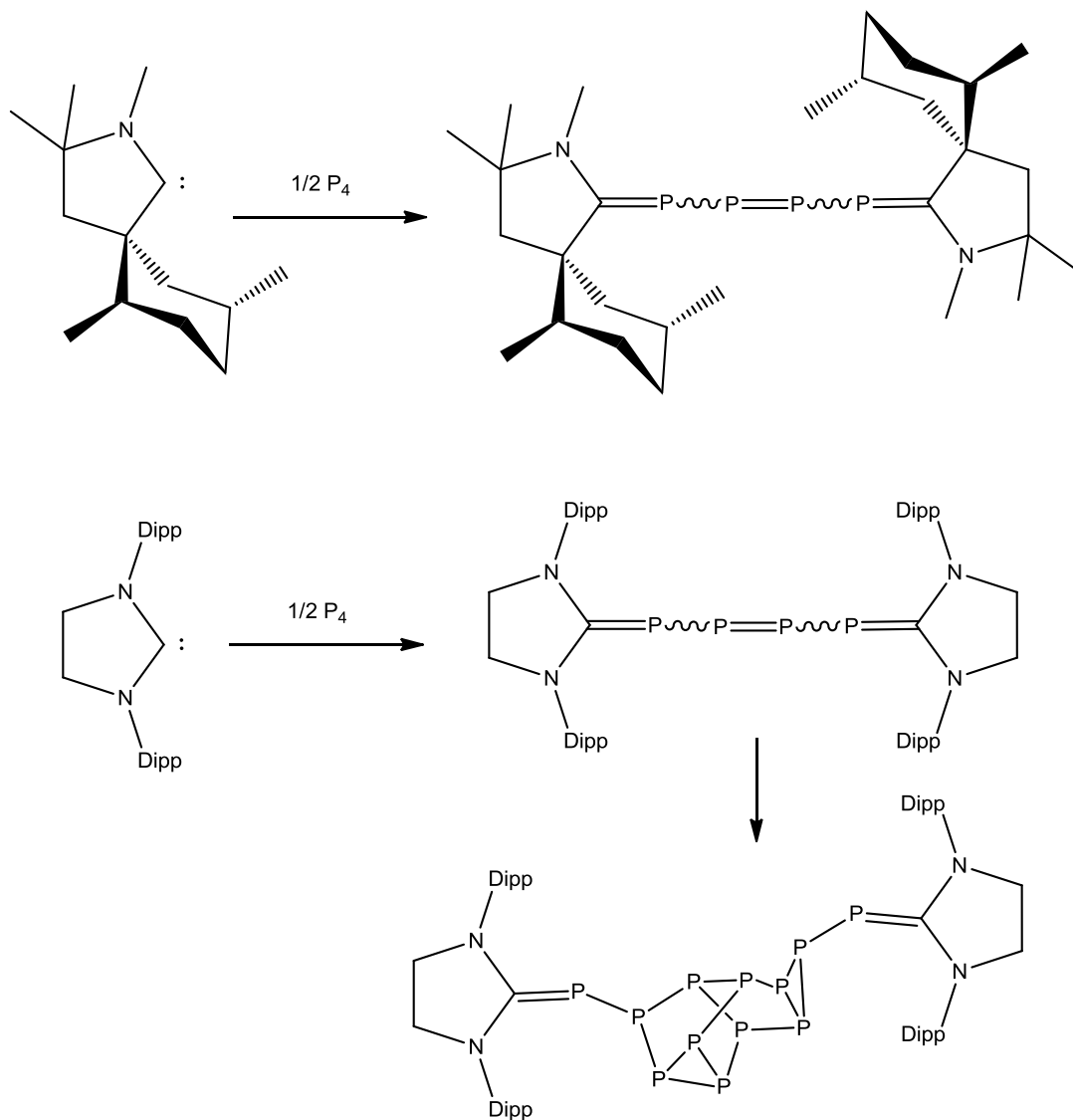


Figure 1.9: NHC-stabilized P(0) complex: NHC(P₁₂)NHC

Other carbenes can be reacted with white phosphorus such as cyclic alkyl amino carbenes (CAAC) and cyclopropylidenes to produce stable species P₁, P₂, P₃, P₄ and higher fragments that include cations and radicals.⁴⁵ Reactions with such carbenes are illustrated in **Scheme 1.15**. The first reaction is the reaction of CAAC with white

phosphorus to give 2,3,4,5-tetraphosphatriene with diastereoselectivity of 9:1 (E to Z).⁴³

The second reaction is of that of a Dipp substituted NHC with white phosphorus to initially give the E and Z isomers of tetraphosphatriene but with time the ³¹P NMR shows evidence of the formation of a P₁₂ cluster as noted above.^{44,45}



Scheme 1.15: Activation of P₄ using CAAC and NHC respectively.

Stabilization of P_2 has been of interest due to the high reactivity of P_2 unlike its lighter N_2 pnictogen counterpart. Robinson's group has been successful in isolating such P_2 fragments. In 2008 Robinson reported the reduction of $NHC(R)PCl_3$ by KC_8 to give the structure shown in **Figure 1.10**. The R group can be an isopropyl group, a mesityl group or a hydrogen. In 2010, Robinson's group found that the reduction of such compounds with lithium results in a carbene-phosphinidene adduct.

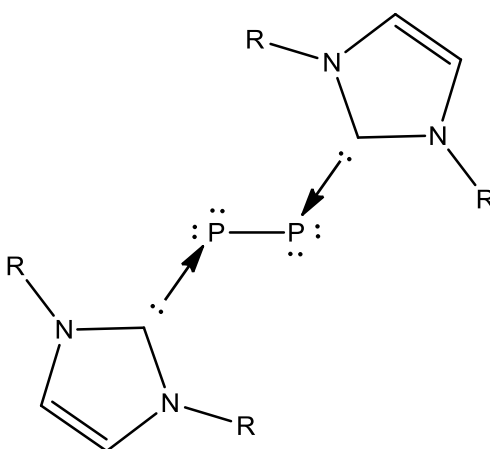
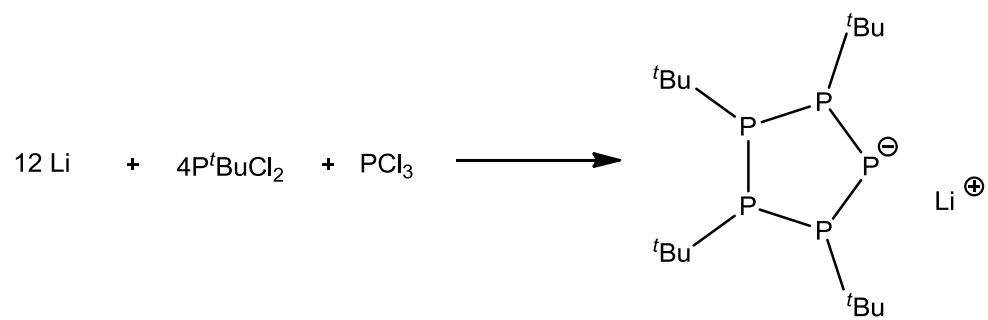


Figure 1.10: Robinson's carbene stabilized di-phosphorus (P_2).

Another advancement in the chemistry of lower oxidation state phosphorus is the preparation of organic cyclic oligophosphanes. Cyclooligophosphanes have been known for quite a long time, dating back to 1877, but the anionic version of these compounds (cyclooligophosphanide anions) have only been known for about 10 years following the work of Baudler *et al.* These phosphanides are prepared by reacting an alkali metal with a dichlorophosphane along with PCl_3 in a ratio of 12:4:1 respectively to give the corresponding cyclooligophosphanes. The reaction scheme is outlined in **Scheme 1.16**.⁴⁶



Scheme 1.16: Synthesis of Li[cyclo—(P₅^tBu₄)]

1.7. Dissertation Overview

The Macdonald group have long been interested in stabilizing main group elements in lower than usual oxidation states. This thesis presents synthetic approaches to stabilizing P^I using cyclic and acyclic *N*-heterocyclic carbenes. Previously, P^I was stabilized by the use of phosphines to give the triphosphenium cation $[(dppe)P^I]^+$, but recently we discovered that the reaction of two equivalents of NHCs with such triphosphenium cation will produce salts containing $[(^R\text{NHC}^{R'})_2P^I]^+$ cations through a ligand replacement mechanism in which the weaker phosphine ligand is displaced by the stronger NHC donors. In this thesis, the improved approach is used to prepare new NHC-stabilized P^I compounds, including cyclic variants. For all of these molecules, the structures, physical properties and important chemical reactivities of these molecules are examined.

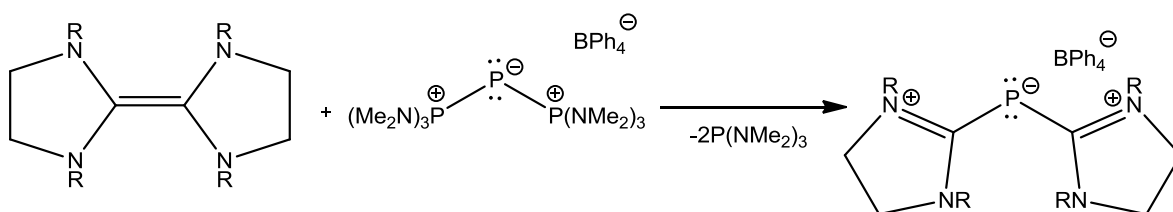
2. Chapter 2 – Acyclic Phosphorus (+1) Stabilization by

N–Heterocyclic Carbenes

2.1. Introduction

After the work of Dimroth on phosphamethine cyanine in 1964, interest in low coordinate phosphorus compounds increased due to the very different chemistry such P–C compounds possess. The synthesis of phosphamethine cyanines involved the use of a suitable chloro-carbon with tris(hydroxymethyl)phosphane or tris(trimethylsilyl)phosphines, which are explosive and pyrophoric reagents, respectively.³⁶⁻³⁸

In 1983, Schmidpeter *et al.* reported that reacting triphosphenium salts with a electron-rich olefin (ERO) gives a di-coordinate P–C compound as illustrated in **Scheme 2.1**. This process involves the insertion of the P atom into the carbon-carbon double bond with the concomitant loss of the phosphine ligands and generates a product that was later described as a P^I center bound by two carbene groups.



Scheme 2.1: Schmidpeter's route to synthesizing P–C di-coordinate compounds.

After the seminal work of Arduengo in 1991 on stable NHCs, great interest was re-initiated in using carbenes to (of the stable and isolable kind) stabilize metal centers as well as main group elements. In 2005 the Macdonald group investigated the effect carbene has on the stabilization of P^I cations and has developed new and convenient approaches to isolate NHC stabilized P^I cations.⁴²

The Macdonald group reported that the reaction of PCl_3 with three equivalents of NHC gave an NHC P^I stable salt.⁴² The major deficiency of this approach is that the by-product chloroimidazolium chloride is hard to separate from the product of interest $[(^R\text{NHC}^{R'})_2P^I][Cl]$ due to the similarities in solubilities of the two salts. Another approach developed by the Macdonald group to obtain the $[(^R\text{NHC}^{R'})_2P^I][Cl]$ product is through a ligand replacement reaction starting with a triphosphenium salt and reacting with an NHC, where the stronger carbene ligand displaces the weaker phosphine ligand, giving the corresponding $[(^R\text{NHC}^{R'})_2P^I]^+$ cation that is easily collected by washing away the phosphine ligand with a non-polar solvent.⁴²

Presented herein is the simple approach to the synthesis and isolation of such $[(^R\text{NHC}^{R'})_2P^I]^+$ cations with high purity. Some important reactivity of these salts is investigated through the use of different oxidation and metal coordination reactions.

2.2. Experimental

General Procedures. All manipulations were carried out using standard inert atmosphere techniques. 1,2-bis(diphenylphosphino)ethane (dppe) and Gold(I) chloride (AuCl) were purchased from Strem Chemicals Inc. and all other chemicals and all other chemicals and reagents were obtained from Aldrich. All reagents were used without further purification. CD₃CN was dried over calcium hydride. All other solvents were dried on a series of Grubbs' type columns and were degassed prior to use.⁴⁷ Cyclic triphosphenium bromide ([dppeP^I][Br]),¹⁷ 1,3,4,5-tetramethylimidazol-2-ylidene²⁷ and 1,3-diethyl-4,5-dimethylimidazol-2-ylidene²⁷ were all synthesized according to literature procedure.

Instrumentation. NMR spectra were recorded at room temperature in CD₃CN solutions on Bruker Avance III 500 MHz, Bruker Avance Ultrashield 300 MHz and Bruker Avance DPX 300 MHz spectrometers. Chemical shifts are reported in ppm relative to external standards (deuterated solvent for ¹H and ¹³C, 85% H₃PO₄ for ³¹P and CFC₃ for ¹⁹F). Coupling constant magnitudes, |J|, are given in Hz. Melting point (Mp) or decomposition points (Dp) were obtained on samples sealed in glass capillaries under dry N₂ using an Electrothermal[®] Melting Point Apparatus. High resolution mass spectrometry and elemental analyses were performed by the University of Windsor Mass Spectrometry Service Laboratory using a Waters Micromass LCT Classic Electrospray Ionization Time of Flight (ESI-TOF) mass spectrometer and a PerkinElmer 2400 combustion CHN analyser, respectively.

Theoretical Methods. All of the computational investigations were performed using the **Compute Canada Shared Hierarchical Academic Research Computing Network**

(SHARCNET) facilities (www.sharcnet.ca) with the Gaussian09⁴⁸ program suite. Geometry optimizations have been calculated using density functional theory (DFT), specifically implementing the PBE1PBE method⁴⁹⁻⁵¹ in conjunction with the TZVP basis set⁵² for all atoms. The geometry optimizations were not subjected to any symmetry restrictions and each stationary point was confirmed to be a minimum having zero imaginary vibrational frequencies. Population analyses were conducted using the Natural Bond Orbital (NBO)⁵³ implementation included with the Gaussian package and the Atoms In Molecules (AIM) analyses⁵⁴ were conducted using AIM2000.^{55,56} Diagrams of calculated structures were generated using Gaussview 3.0.⁵⁷ Summaries of the optimized structures, including electronic energies and Cartesian components for each of the atoms, are detailed in the sections below.

X-ray Crystallography. Crystals were obtained by slow evaporation of the solvent. Crystals were covered in Nujol and placed into a cold stream of N₂ of the Kryo-Flex low temperature device. Data were collected using SMART⁵⁸ software package on a Bruker APEX CCD diffractometer employing graphite-monochromated Mo K α radiation ($\lambda = 0.71073$ Å) source. Hemispheres of data were collected using counting times of 10-30 seconds per frame at -100 °C. The details of crystal data, data collection, and structure refinement are listed in Table 1. Data reductions were performed using the SAINT⁵⁹ software package and the data were corrected for absorption using SADABS.⁶⁰ The structures were solved by direct methods using SIR97⁶¹ and refined by full-matrix least-squares on F^2 with anisotropic displacement parameters for the non-H atoms using SHELXL-97⁶² and the WinGX⁶³ software package and thermal ellipsoid plots were produced using SHELXTL.⁶²

Preparation of $[(^{\text{Me}}\text{NHC}^{\text{Me}})_2\text{P}^{\text{I}}][\text{Br}]$ (1)

To a colorless solution of $[(\text{dppe})\text{P}^{\text{I}}][\text{Br}]$ (1.281 g, 2.516 mmol) in toluene (20 mL) was added an orange/red solution of 1,3,4,5-tetramethylimidazol-2-ylidene (625 mg, 5.032 mmol) in toluene (20 mL). The reaction flask was left to stir overnight and a yellow precipitate was formed that was collected by filtration and washed with Toluene (3 x 20 mL) to remove leftover dppe. The remaining volatiles were removed under reduced pressure to yield a yellow/green product. Recrystallization upon slow evaporation in acetonitrile yielded crystals suitable for analysis by single-crystal X-ray diffraction. Yield: 87% (0.784 g, 2.182 mmol). ^{31}P NMR $\{^1\text{H}\}$ 8 (CD_3CN): -113.63 (s). ^1H NMR (CD_3CN): 2.25 (s, 12H, NCCH_3), 3.49 (s, 12H, NCH_3). $^{13}\text{C}\{^1\text{H}\}$ NMR (CD_3CN): 9.81 (s, NCCH_3), 34.18 (d, NCH_3 , $^3J_{\text{CP}} = 8.15$), 126.52 (s, NCCH_3), 156.70 (d, PCN, $^1J_{\text{CP}} = 88.53$); Mp: 190-193 °C (dec.); Anal. Calc. for $\text{C}_{14}\text{H}_{24}\text{BrN}_4\text{P}$: C, 46.81; H, 6.73; N, 15.60. Found: C, 46.72; H, 7.05; N, 14.99. HRMS-ES Calc. for $\text{C}_{14}\text{H}_{24}\text{N}_4\text{P}^+$: 279.1739, Found: 279.1705.

Preparation of $[(^{\text{Me}}\text{NHC}^{\text{Me}})_2\text{P}^{\text{I}}][\text{BPh}_4]$ (2)

To a yellow solution of $[\text{MeNHCMeP}^{\text{I}}][\text{Br}]$ (100 mg, 0.278 mmol) in tetrahydrofuran (20 mL) was added a colorless solution of $[\text{Na}][\text{BPh}_4]$ (95.3 mg, 0.278 mmol) in tetrahydrofuran (20 mL). The reaction flask immediately turned lighter in color showing both yellow and white precipitate. The solution was allowed to stir for an hour after which volatile components were removed under reduced pressure. Crude residue was dissolved in dichloromethane and precipitate was collected by filtration and washed with dichloromethane (3 x 20 mL). Filtrate was kept and volatile components of the filtrate

were removed under reduced pressure resulting in a yellow/green product. Yield: 96% (160 mg, 0.267 mmol). $^{31}\text{P}\{^1\text{H}\}$ NMR (CD_3CN): -110.74 (s). ^1H NMR (CD_3CN): 1.95 (s, 12H, NCCH_3), 3.11 (s, 12H, NCH_3). $^{13}\text{C}\{^1\text{H}\}$ NMR (CD_3CN): 9.16 (s, NCCH_3), 33.25 (d, NCH_3 , $^3J_{\text{CP}} = 8.08$), 121.60 (s, NCCH_3), 125.47 (s, Ar), 126.15 (s, Ar), 136.15 (s, Ar), 157.22 (d, PCN, $^1J_{\text{CP}} = 90.37$), 164.13 (q, ArCB $^1J_{\text{CB}} = 49.30$).); Mp: 168-169 °C; Anal. Calc. for $\text{C}_{38}\text{H}_{44}\text{BN}_4\text{P}$: C, 76.25; H, 7.41; N, 9.36. Found: C, 76.43; H, 8.09; N, 9.38.

Preparation of [$(^{\text{Me}}\text{NHC}^{\text{Me}})_2\text{P}^{\text{I}}$][OTf] (3)

To a yellow solution of [$(^{\text{Me}}\text{NHC}^{\text{Me}})_2\text{P}^{\text{I}}$][Br] (500 mg, 1.391 mmol) in toluene (20 mL) was added a yellow solution of TMS-triflate (0.3 mL, 1.658 mmol) in toluene (20 mL). The reaction flask immediately turned lighter in color and was allowed to stir for an hour. The resulting yellow to white precipitate was collected by filtration and washed with Toluene (3 x 20 mL). Volatile components were removed under reduced pressure resulting in a pale yellow product. Recrystallization upon slow evaporation in acetonitrile yielded crystals suitable for analysis by single-crystal X-ray diffraction. Yield: 99% (590 mg, 1.377 mmol). $^{31}\text{P}\{^1\text{H}\}$ NMR (CD_3CN): -112.32 (s). $^{19}\text{F}\{^1\text{H}\}$ NMR (CD_3CN): -79.71 (s). ^1H NMR (CD_3CN): 2.19 (s, 12H, NCCH_3), 3.40 (s, 12H, NCH_3). $^{13}\text{C}\{^1\text{H}\}$ NMR (CD_3CN): 9.31 (s, NCCH_3), 34.06 (d, NCH_3 , $^3J_{\text{CP}} = 7.02$), 122.13 (q, CF_3 , $^1J_{\text{CF}} = 318.79$), 127.14 (s, NCCH_3), 158.26 (d, PCN, $^1J_{\text{CP}} = 88.00$); Mp: 144-146 °C; Anal. Calc. for $\text{C}_{15}\text{H}_{24}\text{F}_3\text{N}_4\text{O}_3\text{PS}\cdot\text{CH}_2\text{Cl}_2$: C, 37.44; H, 5.11; N, 10.91. Found: C, 37.38; H, 4.79; N, 10.25.

Preparation of $[(^{\text{Me}}\text{NHC}^{\text{Me}})_2\text{P}^{\text{III}}\text{H}][\text{OTf}]_2$ (4)

To a yellow solution of $[(^{\text{Me}}\text{NHC}^{\text{Me}})_2\text{P}^{\text{I}}][\text{OTf}]$ (100 mg, 0.233 mmol) in toluene (20 mL) was added a yellow solution of triflic acid (0.021 mL, 0.233 mmol) in toluene (20 mL). The reaction was allowed to stir overnight resulting in a solution with white precipitate. The white precipitate was collected by filtration and washed with toluene (3 x 20 mL). Volatile components were removed under reduced pressure resulting in a white product. Yield: 60% (81 mg, 0.140 mmol). Recrystallization upon slow evaporation in acetonitrile yielded crystals suitable for analysis by single-crystal X-ray diffraction. ^{31}P NMR (CD_3CN): -128.62 (d, $^1J_{\text{PH}} = 282.22$). $^{19}\text{F}\{^1\text{H}\}$ NMR (CD_3CN): -78.81 (s). ^1H NMR (CD_3CN): 2.62 (s, 12H, NCCH_3), 3.70 (s, 12H, NCH_3), 6.08 (d, 1H, CPH, $^1J_{\text{PH}} = 282.43$). $^{13}\text{C}\{^1\text{H}\}$ NMR (CD_3CN): 9.50 (s, NCCH_3), 35.34 (d, NCH_3 , $^3J_{\text{CP}} = 5.86$), 121.89 (q, CF_3 , $^1J_{\text{CF}} = 317.71$), 132.98 (s, NCCH_3), 135.39 (d, PCN, $^1J_{\text{CP}} = 37.60$); Mp: $120\text{-}122$ °C; Anal. Calc. for $\text{C}_{16}\text{H}_{25}\text{F}_6\text{N}_4\text{O}_6\text{PS}_2\cdot\text{CH}_2\text{Cl}_2$: C, 30.78; H, 4.10; N, 8.45. Found: C, 30.34; H, 4.03; N, 8.18.

Preparation of $[(^{\text{Me}}\text{NHC}^{\text{Me}})_2\text{P}^{\text{III}}\text{CH}_3]_2[\text{OTf}]$ (5)

To a yellow solution of $[(^{\text{Me}}\text{NHC}^{\text{Me}})_2\text{P}^{\text{I}}][\text{OTf}]$ (100 mg, 0.233 mmol) in toluene (20 mL) was added a clear solution of Methyl Triflate (0.026 mL, 0.233 mmol) in toluene (20 mL). The reaction was allowed to stir overnight resulting in a solution with white precipitate. The white precipitate was collected by filtration and washed with Toluene (3 x 20 mL). Volatile components were removed under reduced pressure resulting in a white product. Yield: 80% (110 mg, 0.186 mmol). ^{31}P NMR (CD_3CN): -55.07 (q, $^1J_{\text{PH}} = 5.95$). $^{19}\text{F}\{^1\text{H}\}$ NMR (CD_3CN): -78.78 (s). ^1H NMR (CD_3CN): 2.26 (s, 12H, NCCH_3), 3.63 (s,

12H, NCH₃), 2.23 (d, 3H, PCH₃, ²J_{PH} = 6.00). ¹³C{¹H} NMR (CD₃CN): 7.81 (d, ¹J_{CP} = 12.91), 9.51 (s, NCCH₃), 35.67 (d, NCH₃, ³J_{CP} = 8.68), 122.14 (q, CF₃, ¹J_{CF} = 320.83), 133.07 (s, NCCH₃), 137.58 (d, PCN, ¹J_{CP} = 42.04); Mp: 171-172 °C; Anal. Calc. for C₁₇H₂₇F₆N₄O₆PS₂·CH₂Cl₂: C, 31.91; H, 4.31; N, 8.27. Found: C, 31.88; H, 4.36; N, 8.92.

Preparation of [(^{Me}NHC^{Me})₂P^VS₂][Br] (6)

To a yellow solution of [(^{Me}NHC^{Me})₂P^I][Br] (100 mg, 0.278 mmol) in dichloromethane (20 mL) was added a yellow solution of Sulfur (S₈) (18 mg, 0.070 mmol) sonicated in dichloromethane (20 mL). The reaction was allowed to stir overnight resulting in a lighter yellow solution. The excess Sulfur was collected by filtration and washed with dichloromethane. Crude residue was sonicated in THF and precipitate was collected by filtration and washed with THF (3 x 20 mL). The remaining volatiles were removed under reduced pressure to yield a white precipitate. Yield: 76% (90 mg, 0.216 mmol). ³¹P{¹H} NMR (CD₃CN): 27.77 (s). ¹H NMR (CD₃CN): 2.26 (s, 12H, NCCH₃), 3.87 (s, 12H, NCH₃). ¹³C{¹H} NMR (CD₃CN): 9.30 (s, NCCH₃), 34.84 (s, NCH₃), 130.40 (s, NCCH₃), 157.22 (d, PCN, ¹J_{CP} = 82.57). Mp: 248 °C (dec.); Anal. Calc. for C₁₄H₂₄BrN₄PS₂: C, 39.72; H, 5.71; N, 13.23. Found: C, 40.02; H, 5.90; N, 12.48. HRMS-ES Calc. for C₁₄H₂₄N₄PS₂⁺: 343.1180, Found: 343.1180.

Preparation of [(^{Me}NHC^{Me})₂P^{III}AuCl][Br] (7)

To a suspension of Au(I)Cl (32 mg, 0.139 mmol) in dichloromethane was added a yellow solution of [(^{Me}NHC^{Me})₂P^I][Br] (50 mg, 0.139 mmol) in dichloromethane (20 mL). The reaction was allowed to stir overnight resulting in a light green solution.

Volatile components were removed under reduced pressure resulting in a green product. Crude residue was sonicated in THF and precipitate was collected by filtration and washed with THF (3 x 20 mL). The remaining volatiles were removed under reduced pressure to yield a wheat colored product. Yield: 55% (45 mg, 0.076 mmol). $^{31}\text{P}\{^1\text{H}\}$ NMR (CD_3CN): -87.06 (s). ^1H NMR (CD_3CN): 2.22 (s, 12H, NCCH_3), 3.68 (s, 12H, NCH_3). $^{13}\text{C}\{^1\text{H}\}$ NMR (CD_3CN): 9.57 (s, NCCH_3), 34.35 (d, NCH_3 , $^3J_{\text{CP}} = 6.87$), 130.37 (s, NCCH_3), 146.27 (d, PCN, $^1J_{\text{CP}} = 60.83$). Mp: dec. at 150°C ; Anal. Calc. for $\text{C}_{14}\text{H}_{24}\text{AuBrClN}_4\text{P}$: C, 28.42; H, 4.09; N, 9.47. Found: C, 30.54; H, 4.61; N, 8.87. HRMS-ES Calc. for $\text{C}_{14}\text{H}_{24}\text{AuClN}_4\text{P}^+$: 511.1093, Found: 511.1086.

Preparation of $[(^{\text{Me}}\text{NHC}^{\text{Me}})_2\text{P}^{\text{V}}(\text{AuCl})_2][\text{Br}]$ (8)

To a suspension of $\text{Au}(\text{I})\text{Cl}$ (62 mg, 0.278 mmol) in dichloromethane was added a yellow solution of $[(^{\text{Me}}\text{NHC}^{\text{Me}})_2\text{P}^{\text{I}}][\text{Br}]$ (50 mg, 0.139 mmol) in dichloromethane (20 mL). The reaction was allowed to stir overnight resulting in a light green solution. Volatile components were removed under reduced pressure resulting in a green product. Crude residue was sonicated in THF and precipitate was collected by filtration and washed with THF (3 x 20 mL). The remaining volatiles were removed under reduced pressure to yield a grey product. Yield: 55% (45 mg, 0.076 mmol). $^{31}\text{P}\{^1\text{H}\}$ NMR (CD_3CN): 31.58 (s). ^1H NMR (CD_3CN): 2.26 (s, 12H, NCCH_3), 3.94 (s, 12H, NCH_3). $^{13}\text{C}\{^1\text{H}\}$ NMR (CD_3CN): 9.79 (s, NCCH_3), 36.19 (d, NCH_3 , $^3J_{\text{CP}} = 6.19$), 132.35 (s, NCCH_3), 145.04 (d, PCN, $^1J_{\text{CP}} = 32.30$). Mp: >320 (dec.) $^\circ\text{C}$; Anal. Calc. for $\text{C}_{14}\text{H}_{24}\text{Au}_2\text{BrCl}_2\text{N}_4\text{P}$: C, 20.40; H, 2.94; N, 6.80. Found: C, 19.14; H, 3.04; N, 4.91. HRMS-ES Calc. for $\text{C}_{14}\text{H}_{24}\text{Au}_2\text{Cl}_2\text{N}_4\text{P}^+$: 743.0447, Found: 743.0439.

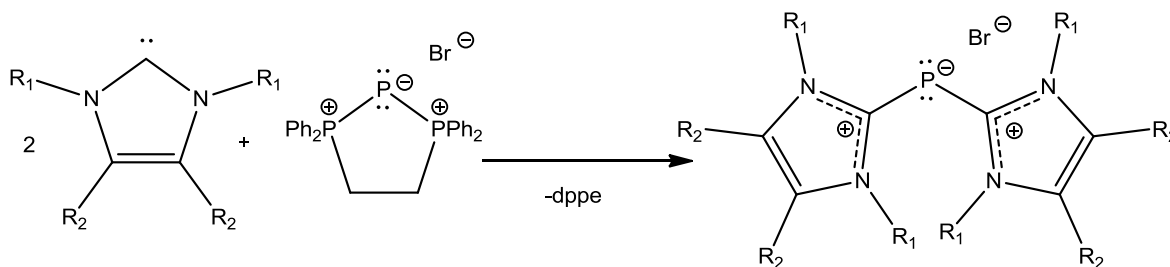
Preparation of $[(^{\text{Et}}\text{NHC}^{\text{Me}})_2\text{P}^{\text{I}}][\text{Br}]$ (9)

To a colorless solution of $[(\text{dppe})\text{P}^{\text{I}}][\text{Br}]$ (167 mg, 0.328 mmol) in toluene (20 mL) was added a red solution of DiethylDimethyl-NHC (100 mg, 0.657 mmol) in toluene (20 mL). The reaction flask was left to stir overnight and a yellow precipitate was formed that was collected by filtration and washed with Toluene (3 x 20 mL) to remove leftover dppe. The remaining volatiles were removed under reduced pressure to yield a yellow/green product. Recrystallization upon slow evaporation in acetonitrile yielded crystals suitable for analysis by single-crystal X-ray diffraction. Yield: 75% (0.102 g, 0.246 mmol). $^{31}\text{P}\{^1\text{H}\}$ NMR (CD_3CN): -128.69 (s). ^1H NMR (CD_3CN): 1.05 (t, 12H, $\text{CH}_3\text{CH}_2\text{N}$, $^3J_{\text{HH}} = 7.20$), 2.20 (s, 12H, NCCH_3), 4.034 (q, 8H, $\text{CH}_3\text{CH}_2\text{N}$, $^3J_{\text{HH}} = 7.20$),. $^{13}\text{C}\{^1\text{H}\}$ NMR (CD_3CN): 9.15 (s, $\text{CH}_3\text{CH}_2\text{N}$), 14.73 (s, NCCH_3), 43.02 (d, $\text{CH}_3\text{CH}_2\text{N}$, $^3J_{\text{CP}} = 6.64$), 127.40 (s, NCCH_3), 156.43 (d, PCN, $^1J_{\text{CP}} = 94.07$). Mp: 180-182 °C (dec.); Anal. Calc. for $\text{C}_{18}\text{H}_{32}\text{BrN}_4\text{P}$: C, 52.05; H, 7.76; N, 13.49. Found: C, 51.83; H, 7.72; N, 13.15.

2.3. Results and Discussions

2.3.1. Synthesis

As illustrated by the earlier work of Macdonald *et al.*, the reaction of 2 equivalents of Kuhn's stable NHCs with triphosphenium salts results in the displacement of the bis(diphenylphosphino)ethane (dppe) ligand by the stronger carbene donor ligand.⁴² Previously, the Macdonald group was successful in characterizing $[(^{\text{iPr}}\text{NHC}^{\text{Me}})_2\text{P}^{\text{I}}][\text{Cl}]$ and this chapter presents the preparation of other derivatives such as $[(^{\text{Me}}\text{NHC}^{\text{Me}})_2\text{P}^{\text{I}}][\text{Br}]$ and $[(^{\text{Et}}\text{NHC}^{\text{Me}})_2\text{P}^{\text{I}}][\text{Br}]$. The method of synthesis we used is an alternative synthetic approach to the direct PCl_3 reduction. As indicated above, in the latter case, a chloroimidazolium chloride by-product is formed which is hard to separate from the desired product ($[(^{\text{R}}\text{NHC}^{\text{R'}})_2\text{P}^{\text{I}}][\text{Br}]$) due to the similarity in the solubility of the product and the by-product. Thus, by employing the ligand displacement approach, the displaced dppe is easily washed away with non-polar solvents such as pentane or toluene allowing for the isolation of high-purity materials that are often crystalline.



Scheme 2.2: Synthesis of $[(^{\text{Me}}\text{NHC}^{\text{Me}})_2\text{P}^{\text{I}}][\text{Br}]$.

Bromide salts of cations of the form $[(^{\text{R}}\text{NHC}^{\text{R'}})_2\text{P}^{\text{I}}]^+$ are generally prepared by first starting with the triphosphenium salt $[(\text{dppe})\text{P}^{\text{I}}][\text{Br}]$ in THF or toluene in a Schlenk

flask under nitrogen. To the suspended a solution containing two equivalents of the corresponding $^R\text{NHC}^{R'}$ is cannulated. The reaction mixture immediately turns yellowish in colour and is left to stir for a few hours before collecting the product. The precipitate in the solution is the desired product $[(^R\text{NHC}^{R'})_2\text{P}^I][\text{Br}]$ which is collected by filtration; while the displaced dppe side product is washed away using pentane or toluene (Scheme 2.2).

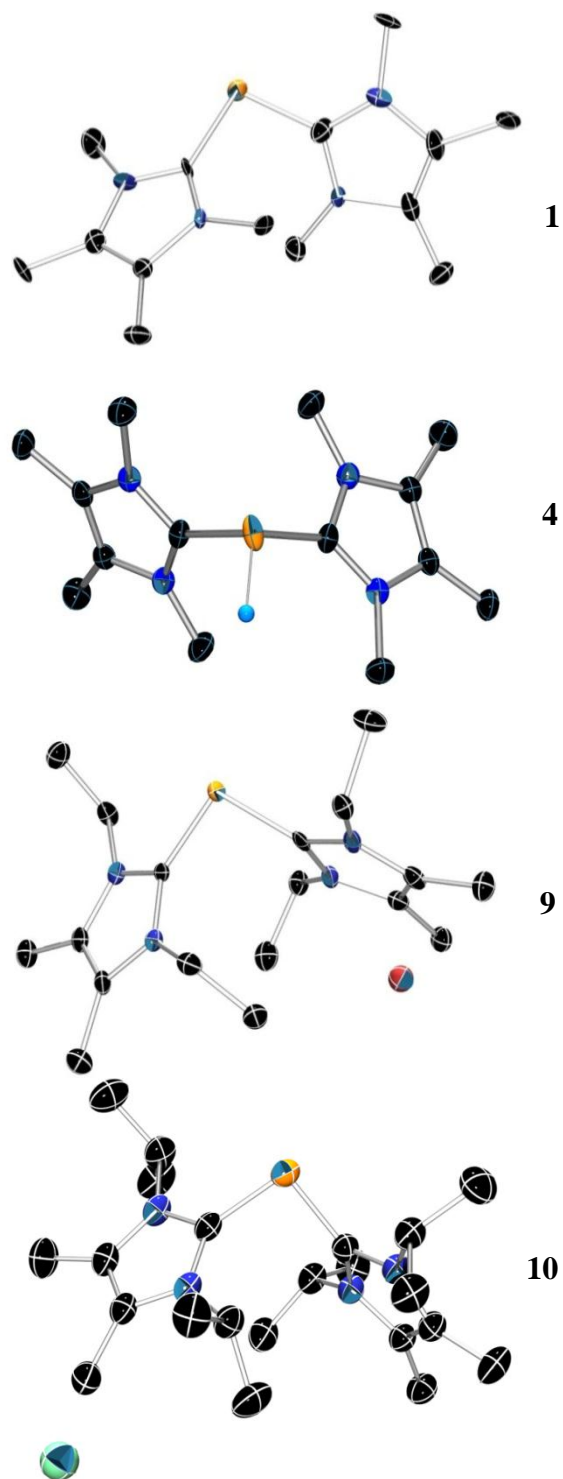


Figure 2.1: Thermal ellipsoid plots of the molecular structures of compounds **1**, **4**, **9** and **10**⁴².

Compound	$[(^{\text{Me}}\text{NHC}^{\text{Me}})_2\text{P}^{\text{I}}][\text{Br}]$	$[(^{\text{Me}}\text{NHC}^{\text{Me}})_2\text{P}^{\text{I}}\text{H}][\text{OTf}]_2$	$[(^{\text{Et}}\text{NHC}^{\text{Me}})_2\text{P}^{\text{I}}][\text{Br}]$
Compound ID	CMAS4 (1)	CMAS8 (4)	CMAS10 (9)
Empirical formula	$\text{C}_{14}\text{H}_{24}\text{BrN}_2\text{P}$	$\text{C}_{16}\text{H}_{25}\text{F}_6\text{N}_4\text{O}_6\text{PS}_2$	$\text{C}_{18}\text{H}_{33}\text{BrN}_4\text{P}$
Formula weight	331.23	578.49	429.04
Temperature	173(2) K	173(2) K	173(2) K
Wavelength	0.71073 Å	0.71073 Å	0.71073 Å
Crystal system	Monoclinic	Monoclinic	Rhombohedral
Space group	P2(1)/c	C2/c	R3
a (Å)	6.9665(13) Å	a = 8.8801(15)	a = 12.1188(9)
b (Å)	12.104(2) Å	b = 13.671(2)	b = 12.1188(9)
c (Å)	22.873(4) Å	c = 19.655(3)	c = 12.1188(9)
α (°)	90	90	98.79
β (°)	98.329(3)	97.227(3)	98.79
γ (°)	90	90	98.79
V (Å ³)	1908.3(6)	2367.2(7)	1709.8(2)
Z	4	4	3
Density (calculated) g·cm ⁻³	1.153	1.623	1.250
Absorption coefficient mm ⁻¹	2.227	0.381	1.883
F(000)	688	1192	676
Crystal size mm	0.40 x 0.30 x 0.20	0.40 x 0.30 x 0.30	0.30 x 0.30 x 0.20
Theta range for data collection (°)	1.80 to 27.50°.	2.09 to 27.50°.	2.21 to 27.49°.
Index ranges	-8 ≤ h ≤ 3 -15 ≤ k ≤ 15 -28 ≤ l ≤ 29	-11 ≤ h ≤ 10 -17 ≤ k ≤ 17 -24 ≤ l ≤ 16	-15 ≤ h ≤ 14 -15 ≤ k ≤ 15 -15 ≤ l ≤ 14
Reflections collected	10524	6993	14889
Independent reflections	4065 [R(int) = 0.0856]	2540 [R(int) = 0.0534]	4758 [R(int) = 0.0749]
Completeness to theta max	93.00%	93.10%	93.90%
Absorption correction	"multi-scan" semi-empirical correction done with SADABS	"multi-scan" semi-empirical correction done with SADABS	"multi-scan" semi-empirical correction done with SADABS
Max. and min. transmission	0.638 and 0.325	0.892 and 0.687	0.686 and 0.494
Refinement method	Full-matrix least-squares on F ²		
Data / restraints / parameters	4065 / 0 / 216	2540 / 1 / 167	4758 / 1 / 236
Goodness-of-fit on F ²	1.258	1.059	0.965
Final R indices [I > 2σ(I)]	R1 = 0.1475 wR2 = 0.3296	R1 = 0.0778 wR2 = 0.1723	R1 = 0.0484 wR2 = 0.0732
R indices (all data)	R1 = 0.1878 wR2 = 0.3471	R1 = 0.1089 wR2 = 0.1934	R1 = 0.0600 wR2 = 0.0779
Largest diff. peak and hole (e·Å ⁻³)	1.673 and -1.904	0.594 and -0.517	0.350(9)

Table 2.1: Summary of crystallographic data for compounds **1**, **4** and **9**.

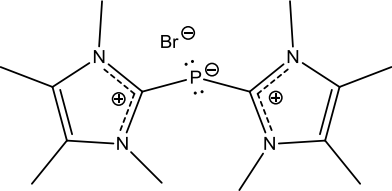
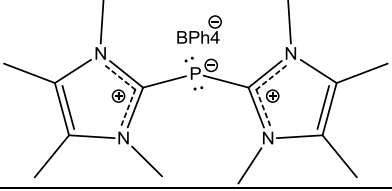
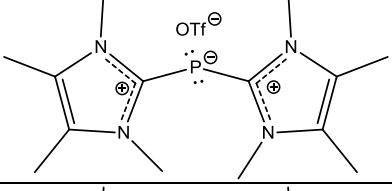
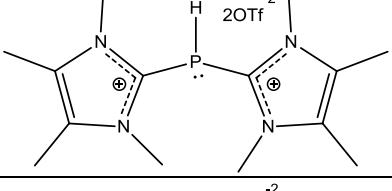
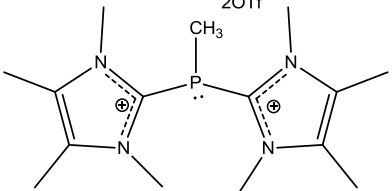
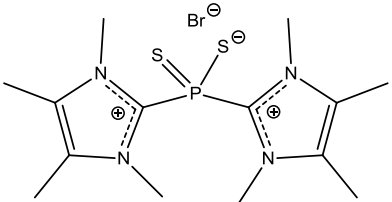
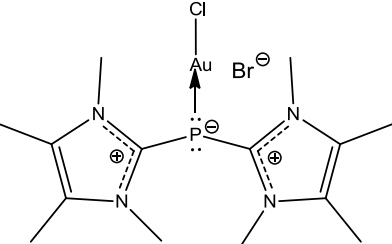
Compound	C–P Bond Distance (Å)	C–P–C Bond Angle (°)	N–C–P–C Dihedral Angle (°)
1	1.807(6) [*] – 1.809(7)	99.2(3)	42.1(7) – 43.5(7)
4	1.8567(2) – 1.8596(2)	99.54(1)	55.32(3) – 78.77(3)
9	1.8345(2) – 1.8358(3)	96.99(2)	58.49(3) – 61.52(3)

^{*} Numbers in parenthesis show estimated standard deviation (esd) which indicates the precision in the last digit.

Table 2.2: Metrical parameters of the crystal structures **1**, **4** and **9**.

Figure 2.1 shows the crystal structures of compounds **1**, **4**, **9** and **10**. Crystallographic data and metrical parameters are listed in **Tables 2.1** and **2.2** respectively. Comparing the C–P bond distances in **1** to the C–P bond distances in **4**, the C–P bond in **1** is shorter than that in **4** which indicates that this bond is a stronger bond suggesting the involvement of multiple-bonding (or at least delocalization of the π -system) in the P^I model. More about C–P bond delocalization is discussed in the computational section of this chapter. The Lewis structure and ³¹P NMR chemical shifts of all compounds are listed in **Table 2.3** in the section below.

2.3.2. NMR Analysis

Structure	Compound	^{31}P δ^a
	$[(^{\text{Me}}\text{NHC}^{\text{Me}})_2\text{P}^{\text{I}}][\text{Br}]$ (1)	-113.6
	$[(^{\text{Me}}\text{NHC}^{\text{Me}})_2\text{P}^{\text{I}}][\text{BPh}_4]$ (2)	-110.7
	$[(^{\text{Me}}\text{NHC}^{\text{Me}})_2\text{P}^{\text{I}}][\text{OTf}]$ (3)	-112.3
	$[(^{\text{Me}}\text{NHC}^{\text{Me}})_2\text{P}^{\text{III}}\text{H}][\text{OTf}]_2$ (4)	-128.6 (d)
	$[(^{\text{Me}}\text{NHC}^{\text{Me}})_2\text{P}^{\text{I}}\text{CH}_3][\text{OTf}]_2$ (5)	-55.0 (q)
	$[(^{\text{Me}}\text{NHC}^{\text{Me}})_2\text{P}^{\text{V}}\text{S}_2][\text{Br}]$ (6)	27.8
	$[(^{\text{Me}}\text{NHC}^{\text{Me}})_2\text{P}^{\text{III}}\text{AuCl}][\text{Br}]$ (7)	-87.1

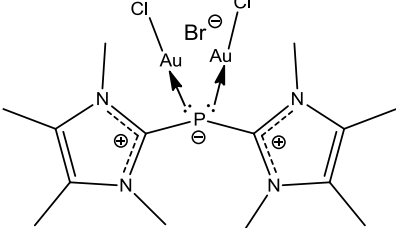
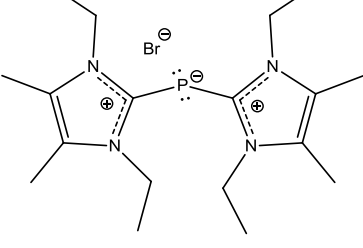
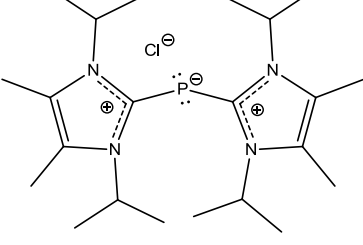
	$[(^{\text{Me}}\text{NHC}^{\text{Me}})_2\text{P}^{\text{V}}(\text{AuCl})_2][\text{Br}]$ (8)	-31.6
	$[(^{\text{Et}}\text{NHC}^{\text{Me}})_2\text{P}^{\text{I}}][\text{Br}]$ (9)	-128.7
	$[(^{\text{iPr}}\text{NHC}^{\text{Me}})_2\text{P}^{\text{I}}][\text{Br}]$ (10)	-124.2 ⁴²

Table 2.3: Structures and ^{31}P NMR data of acyclic $(^{\text{R}}\text{NHC}^{\text{R}'})_2\text{P}^{\text{I}}$ compounds.

$[(^{\text{Me}}\text{NHC}^{\text{Me}})_2\text{P}^{\text{I}}][\text{Br}]$ **1** and $[(^{\text{Et}}\text{NHC}^{\text{Me}})_2\text{P}^{\text{I}}][\text{Br}]$ **9** were both synthesized in high yields and were characterized using NMR, X-ray crystallography and elemental analysis. ^{31}P NMR chemical shifts reported for such products (through the ligand displacement approach) were in the range of -127 to -124 ppm.⁴² The ^{31}P NMR collected for **1** gave a singlet at -113.63 ppm which is in the region of what is anticipated for these compounds but a little bit less shielded than that observed for the variants containing larger alkyl groups. Comparing the tetramethyl product to the diethyldimethyl product, the diethyldimethyl gave a value of -128.69 ppm which is basically in range of what is expected.

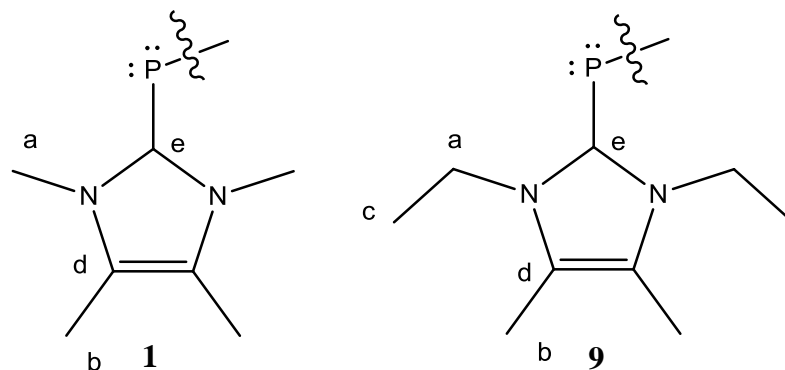
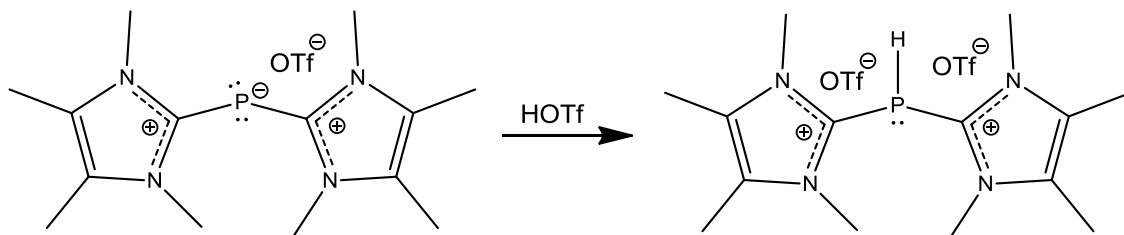


Figure 2.2: Labeling of protons and carbons in **1** and **9**.

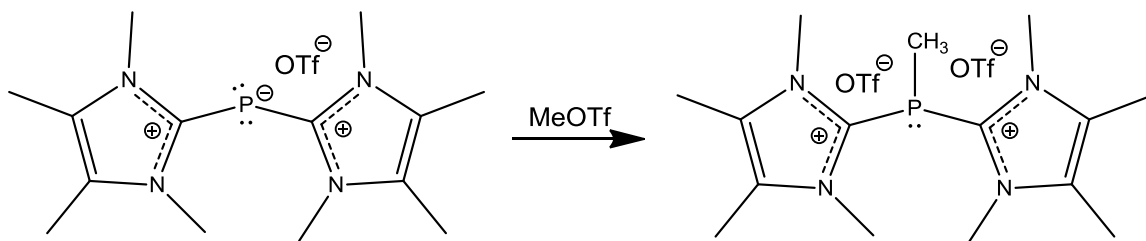
The ^1H NMR of **1** gave two singlets: **a** and **b**; while the ^1H NMR of **9** gave three peaks, a quartet, a singlet and a triplet: corresponding to **a**, **b** and **c**, respectively. The protons on **a** are more deshielded than the protons on the methyl backbone (**b**). This is likely because nitrogen is more electronegative and thus it withdraws electron density from the protons and renders them less shielded. The ^{13}C NMR gives a distinctive doublet for **e** with a $^1J_{\text{PC}}$ coupling constant of 88.5 Hz in **1** and 94.1 Hz in **9**. A smaller doublet is observed for **a** with a $^3J_{\text{PC}}$ coupling constant of about 8-9 Hz. Anion exchange does not change the NMR chemical shifts of the cation significantly but it does alter other properties of the salt such as solubility and melting point.

The electron-rich nature of the dicoordinate phosphorus atom in the salts prepared above suggested that the compounds should be susceptible to protonation and oxidation. In order to access the salts behaviour with regard to protonation and methylation, their reaction with triflic acid and methyl triflate, respectively, were examined. We reasoned that it would be wise to use P^{I} salts of the same triflate anion in order to minimize complications that may arise from preparing products with mixed anions. Furthermore, we found that the addition of triflic acid directly to the bromide salt did not result in the

desired product; this result can be attributed to the presence of the bromide anion, which can allow for alternative reactions. In contrast, the treatment of the triflate salt $[(^{\text{Me}}\text{NHC}^{\text{Me}})_2\text{P}^{\text{I}}][\text{OTf}]$ gave the anticipated protonated product; methylation with MeOTf worked similarly (**Schemes 2.3 and 2.4 respectively**).



Scheme 2.3: Synthesis of $[(^{\text{Me}}\text{NHC}^{\text{Me}})_2\text{P}^{\text{I}}\text{H}][\text{Br}]$.

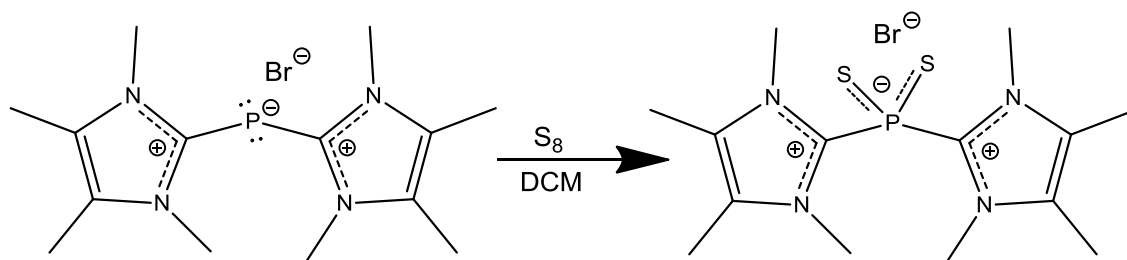


Scheme 2.4: Synthesis of $[(^{\text{Me}}\text{NHC}^{\text{Me}})_2\text{P}^{\text{I}}\text{CH}_3][\text{Br}]$.

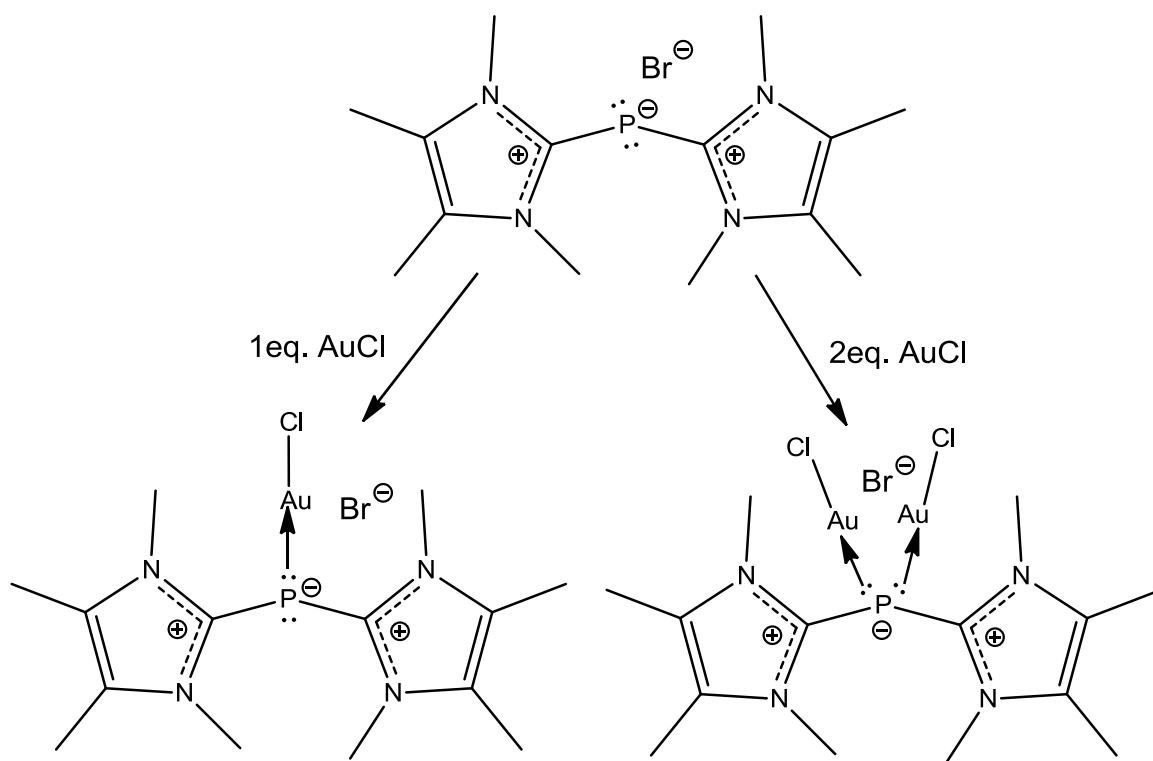
In both protonation and methylation reactions, the resultant product was white in colour, which suggests that oxidation of the phosphorus did indeed take place. The resultant protonated salt $[(^{\text{Me}}\text{NHC}^{\text{Me}})_2\text{P}^{\text{I}}\text{H}][\text{OTf}]_2$ **4** features a doublet in the proton-coupled ^{31}P NMR spectrum with a $^1J_{\text{PH}}$ coupling constant of 282 Hz. Similarly the methylated variant $[(^{\text{Me}}\text{NHC}^{\text{Me}})_2\text{P}^{\text{I}}\text{CH}_3][\text{OTf}]_2$ **5** gave a quartet with a $^2J_{\text{PH}}$ coupling constant of ca. 6 Hz. In terms of changes in the ^{31}P NMR chemical shift with respect to

the starting salt, the resonance for the protonated phosphorus dication is more shielded while the signal for methylated phosphorus is less shielded. The P–H coupling constants observed in the ^{31}P NMR were confirmed in the corresponding proton NMR spectra. The ^1H NMR spectrum of **4** contains a doublet at 6.08 ppm with a $^1J_{\text{PH}}$ of 282 Hz while the ^1H NMR of **5** gave a doublet at 2.23 ppm with a $^2J_{\text{PH}}$ of 6 Hz. Moreover, the ^{13}C NMR spectra contained distinctive small doublet with a $^1J_{\text{CP}}$ of 38 Hz for **4** and a $^1J_{\text{CP}}$ of 42 Hz for **5**. It should be noted that the attempted oxidation of either of the P^{III} centers in **4** or **5** with a second methyl cation or proton was not successful and the rationale for this non-reactivity is discussed in the computational section later on this chapter.

Oxidation with sulfur (**Scheme 2.5**) and metal coordination reactions were performed and confirmed by NMR, Mass Spec and Elemental Analysis. Oxidation with sulfur (**6**) gave a ^{31}P NMR singlet at 27.77 ppm, while single (**7**) and double (**8**) Au(I)Cl coordination gave singlet peaks at –87.06 ppm and 31.58 ppm respectively (**Scheme 2.6**). As the case with protonation and methylation, sulfonation and metal coordination both also gave lighter coloured products than the yellow starting material which can also be used as indicator for the oxidation of the phosphorus center. In terms of the proton NMR spectra, the two singlet signals observed for the product and are almost indistinguishable from those of the starting material. The ^{13}C NMR spectrum featured the small doublets that arise from the carbon atoms directly bonded to the phosphorus. $^1J_{\text{PC}}$ coupling constants were 83 Hz, 61 Hz and 32 Hz for **6**, **7** and **8** respectively. One thing to note is that the observed coupling for the oxidized phosphorus center is large in comparison to the other P^{V} metal coordinated center.



Scheme 2.5: Synthesis of $[(^{\text{Me}}\text{NHC}^{\text{Me}})_2\text{P}^{\text{V}}\text{S}_2][\text{Br}]$.



Scheme 2.6: Synthesis of $[(^{\text{Me}}\text{NHC}^{\text{Me}})_2\text{P}^{\text{I}}\text{AuCl}][\text{Br}]$ and $[(^{\text{Me}}\text{NHC}^{\text{Me}})_2\text{P}^{\text{I}}(\text{AuCl})_2][\text{Br}]$

2.3.3. Mass Spec Analysis

High Resolution Mass Spec (HRMS-ES) was performed on the three samples: **6**, **7** and **8**. As for **6**, the m/z value found of 343.1180 Da as shown in **Figure 2.3a** is exactly what was calculated (343.1180 Da). As for **7** and **8**, the results were interesting in that they confirm that halide exchange had occurred as illustrated by the data in **Table 2.3**. In particular, the m/z values calculated for **7** and **8** would be based on the molecular formula $C_{14}H_{24}AuClN_4P^+$ and $C_{14}H_{24}Au_2Cl_2N_4P^+$ respectively. For **7**, the molecular formula expected is observed as shown in **Figure 2.3b**, but there were also peaks that indicate the presence of $C_{14}H_{24}AuBrN_4P^+$ (**Figure 2.3c**). Similarly for **8**, $C_{14}H_{24}Au_2Cl_2N_4P^+$ was observed (**Figure 2.3d**) as was $C_{14}H_{24}Au_2BrClN_4P^+$ (**Figure 2.3e**) and $C_{14}H_{24}Au_2Br_2N_4P^+$ (**Figure 2.3f**).

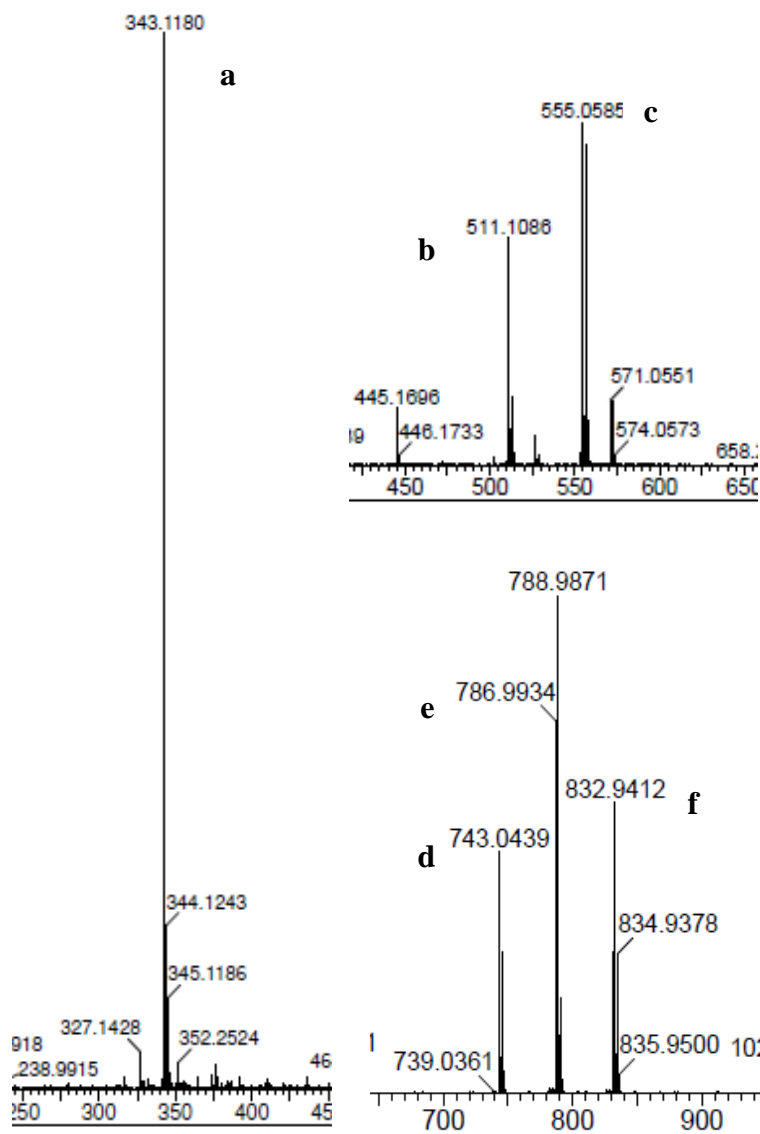


Figure 2.3: Mass Spectra of **6**, **7** and **8**. (Electrospray ionization)

Molecular Formula	Calculated (Da)	Found (Da)[*]
C₁₄H₂₄S₂N₄P⁺	343.1180	343.1180
C₁₄H₂₄AuClN₄P⁺	511.1093	511.1086
C₁₄H₂₄AuBrN₄P⁺	555.0588	555.0585
C₁₄H₂₄Au₂Cl₂N₄P⁺	743.0447	743.0439
C₁₄H₂₄Au₂BrClN₄P⁺	786.9942	786.9934
C₁₄H₂₄Au₂Br₂N₄P⁺	832.9416	832.9412

^{*}(Electrospray Method)

Table 2.4: Calculated and found Mass Spec values for **6**, **7** and **8**.

2.3.4. Computational Studies

In an attempt to rationalize the observed features and reactivity of the synthesized compounds, computational studies were performed to provide insight into the bonding, electronic features, reactivity and structural features of these compounds. Thus we used DFT calculations to optimize the geometries of a series of relevant model compounds and probed their properties.

Compound	C–P Bond Distance (Å)	C–P–C Bond Angle (°)	N–C–P–C Dihedral Angle (°)
1'	1.81149, 1.81152	99.30	47.82 – 47.89
4'	1.84208, 1.84105 P–H: 1.41678	104.71	55.82 – 78.01
5'	1.84601, 1.85046 P–CH ₃ : 1.84074	103.30	50.08 – 78.46
6'	1.88507, 1.88508 P–S: 1.96706	98.03	51.65 – 51.66
7'	1.84627, 1.84576 P–Au: 2.29861	98.35	50.78 – 60.87
8'	1.85464, 1.85464 P–Au: 2.27822, 2.27822	99.65	54.95 – 54.95
9'	1.81570, 1.81557	100.38	48.49 – 48.65
10'	1.82689, 1.82689	100.19	55.60 – 55.62

Table 2.5: Bond distances and angles. DFT (PBE1PBE/TZVP)

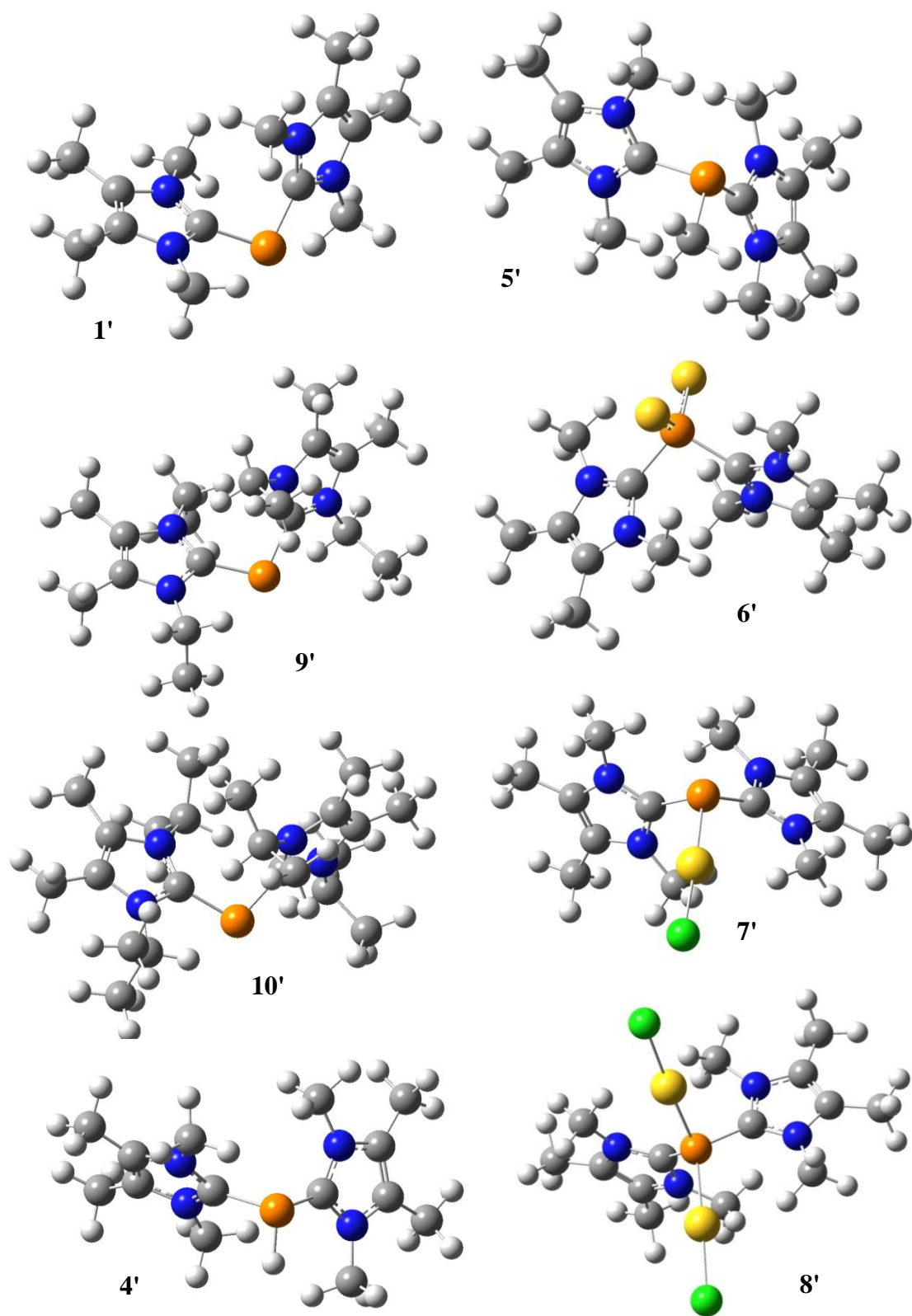


Figure 2.4: Geometry-optimized structures for model compounds **1'**, **4'-10'**. DFT (PBE1PBE/TZVP)

The optimized structure for the model compound **1'** reproduced the features observed in the structure of the cation in **1** very well and attests to the suitability of the theoretical method we used. This can be confirmed by comparing results obtained for compounds **1'**, **4'** and **9'** in **Table 2.5** to **1**, **4** and **9** in **Table 2.1**. The pertinent data collected in **Table 2.5** reveals many important insights. For example, in comparing the C–P bond distances in **1'** to the C–P bond distances in **4'-8'**, one realizes that **1'** has a considerably shorter bond length which indicates that this bond is a stronger bond suggesting the involvement of multiple-bonding (or at least delocalization of the π -system) in the P^I model in comparison to the bonds in the P^{III} and P^V models. This interpretation is reinforced by analyzing the role of the second lone pair in the π -system of the molecule (see below).

Compound	Symmetry	HOMO (eV)	LUMO (eV)	HOMO-LUMO Gap (eV)
1'	C ₁	−8.17	−3.67	4.50
4'	C ₁	−13.41	−8.05	5.36
5'	C ₁	−13.18	−7.88	5.30
6'	C ₁	−9.09	−4.29	4.80
7'	C ₁	−9.04	−4.41	4.63
8'	C ₁	−9.59	−4.97	4.61
9'	C ₁	−7.95	−3.72	4.23
10'	C ₁	−7.83	−3.50	4.33

Table 2.6: Energy gap calculations. DFT (PBE1PBE/TZVP)

Looking at the frontier orbital energies (HOMO and LUMO) energies and HOMO-LUMO gaps (**Table 2.6**) of these different compounds, one realizes that protonation and methylation of the P^I center have the greatest effect on changing the HOMO-LUMO energies of the starting material model **1'** (the un-oxidized compound). The protonated and methylated compounds (**4'** and **5'** respectively) have a bigger HOMO-LUMO gap than what is calculated for **1** which would mean that the compound is less reactive and thus, more stable. The much lower HOMO energies also suggest that the lone pairs on the phosphorus of compounds **4** and **5** are much more resistant to oxidation which is consistent with the experimental observations: all attempts to further oxidize **4** or **5** did not give the anticipated doubly protonated or doubly methylated compounds simply because the lone pair on the phosphorus is stable and is hard to oxidize. DFT (PBE1PBE/TZVP) calculations showed that single protonation has an enthalpy of -695 kJ mol^{-1} , while second protonation step gave -195 kJ mol^{-1} . This number is in the gas phase and is comparable to proton affinities of typical solvents meaning that under normal conditions, the solvent would get protonated before getting the second protonation step to take place. Other reactions like the oxidation with sulfur to produce **6'** and metal coordination (to generate **7'** and **8'**) change the HOMO-LUMO gap slightly but the numbers are still comparable to those of **1'**. Comparing compound **7** to **4** and **5**, one realizes that the HOMO-LUMO gap of **7** is smaller and the absolute energy of the HOMO is comparable to **1** which renders the coordination of a second Au(I)Cl possible; again, this is consistent with the behavior that was observed in practice in the preparation of **8**.

Compound	NBO* Charge on Phosphorus	P–C WBI	C–N WBI	C–N WBI
1'	0.13769	1.0894	1.2342	1.2163
4'	0.55234	0.9474	1.2790	1.2619
5'	0.77724	0.9402	1.2791	1.2719
6'	0.98285	0.7174	1.2939	1.2692
7'	0.25278	1.0152	1.2593	1.2514
8'	0.30977	0.9559	1.2737	1.2650
9'	0.11163	1.0587	1.2480	1.2409
10'	0.08641	1.0528	1.2494	1.2365

* Natural Bond Orbital (NBO) is a calculated bonding orbital showing maximum electron density.

Table 2.7: NBO WBI values for the model complexes. DFT (PBE1PBE/TZVP)

Table 2.7 shows the Wiberg Bond Indices (WBI) which are quantities that we can use to gain a better understanding of the phosphorus-carbene bonding in oxidized and un-oxidized compounds. Among the un-oxidized compounds, **9'** and **10'** are very comparable while **1'** is significantly larger. Compound **1'** has a greater WBI which can be attributed to the more co-planar arrangement of the carbene ligands within the molecule (and with the C-P-C plane). The tetramethyl carbene is a smaller, less sterically-bulky carbene which affords a more planar structure and thus, greater conjugation can occur resulting in a greater bond order. Lower bond orders are observed in the oxidized compounds simply because they do not have a π -type lone pair with appropriate symmetry to interact with π -system of the carbene fragments.

Compound	1 st Lone Pair Population on Phosphorus	2 nd Lone Pair Population on Phosphorus	1 st Lone Pair Population on Nitrogen	2 nd Lone Pair Population on Nitrogen	Interaction of 2 nd Lone Pair of Phosphorus with C–N bond (kcal/mol)
1'	1.92712	1.52752	1.53822	1.53817	61.77, 61.74
4'	1.91330	N/A	1.49169	1.48279	N/A
5'	1.88974	N/A	1.50319	1.49346	N/A
6'	N/A	N/A	1.50768	1.50770	N/A
7'	1.85279	N/A	1.51849	1.50743	N/A
8'	N/A	N/A	1.50206	1.50206	N/A
9'	1.92356	1.53866	1.53760	1.53782	62.23, 62.42
10'	1.91928	1.62174	1.52739	1.52743	31.99, 32.01

Table 2.8: Lone pair population and interaction. DFT (PBE1PBE/TZVP)

To further elucidate the role played by the second lone pair of phosphorus in the π -system(s) within the models, the population and interactions of the second lone pair have been calculated for each of the un-oxidized model compounds. In terms of the population, the first lone pair has a value close to 2, which is indicative of minimal contribution to the π -system: this is the σ -type lone pair. The second lone pair gave a value of about 1.5 for the dimethyl and diethyl compounds and 1.6 for the diisopropyl model compound. These populations indicate that the second lone pair on the phosphorus contributes to the π -system and is not fully localized on the phosphorus center. Looking at the NBO hybrid orbitals calculated for the three compounds (**1'**, **9'** and **10'**), the first lone pair is about 70% s-character and 30% p-character for all three. The second lone pair

however, is more than 99.8% p-character. The presence of this lone pair in the π -system allows for electron density to be donated into the P–C bond (to generate bond orders that are greater than 1) which would also be delocalized with the C–N bond of the carbene fragments.

It is the presence of the π -type lone pair that allows the π -system to extend throughout the molecule and allows the compounds to absorb light in the visible region. This chromophore gives the compounds the yellow colour that is lost upon oxidation of the molecules. The interaction of the second π -type lone pair and the C–N bond is confirmed by the NBO analyses. In the dimethyl and diethyl model compounds, one can see that the population and interaction values are relatively close to each other. In contrast, the interaction in the isopropyl model compound, which has bulkier substituents and features a less-coplanar arrangement, is about half that of the dimethyl or diethyl compounds. Less interaction is further reflected in the lone pair having greater population on the phosphorus and thus less contribution.

Compound	$\lambda_1/\lambda_{\text{max}}$ (nm)	λ_2 (nm)	λ_3 (nm)
1'	351.08	311.76	—
4'	277.90	259.32	248.16
5'	281.63	257.40	245.09
6'	330.64	328.06	315.35
9'	382.47	316.06	291.49
10'	380.11	336.06	293.48

Table 2.9: Time dependent (TD) calculations. TD-DFT (PBE1PBE/TZVP)

The un-oxidized acyclic compounds are yellow in colour, while the oxidized acyclic compounds lose the yellow colour and are colourless. Normally, the greater the extent of conjugation in a system, the lower the HOMO-LUMO gap and thus, the lower the energy required for excitation of an electron. A lower energy gap is reflected by a higher wavelength (λ) as they are inversely proportional in the equation:

$$E = \frac{hc}{\lambda}$$

Looking back at the data in **Table 2.6**, the HOMO-LUMO gap is found to be greater for oxidized compounds, especially for compounds **4** and **5**. Similarly, the data in **Table 2.9** show that protonation and methylation show the greatest deviation from the un-oxidized compound just as the case in the HOMO-LUMO gap. This decrease in wavelength after oxidation of the phosphorus explains the loss of colour observed due to the loss of the extended conjugation.

2.4. Conclusions

Various derivatives of the acyclic $[(^R\text{NHC}^{R'})_2\text{P}^I]^+$ cations containing different R groups (Me and Et) and different anions such as triflate (OTf) and tetraphenylborate (BPh₄) has been synthesized. This was achieved by a ligand replacement reaction where the stronger $^R\text{NHC}^{R'}$ carbene replaces the weaker dppe ligand. This approach is a cleaner, more effective approach than the direct reduction of PCl_3 .⁴²

$[(^R\text{NHC}^{R'})_2\text{P}^I]^+$ cations featured a shorter P–C bond distance than its oxidized variants. This suggested that the second lone pair on the phosphorus played an important role in the π -system of the molecule inducing multiple bonding in the P–C bond. This was confirmed by computational methods where WBI calculation showed that an unoxidized $[(^R\text{NHC}^{R'})_2\text{P}^I]^+$ cation has a bond order greater than 1. Interaction of the second lone pair with the imidazolium C–N bond has been calculated and showed to be significant (32 and 62 kcal/mol).

Oxidation reactions were performed to study the reactivity of these compounds. Single protonation and methylation were successful, but adding a second proton or methyl to the phosphorus center was not possible. Having an inert lone pair was explained by the computational calculations where the protonated and methylated compounds gave a bigger HOMO-LUMO gap making the lone pair stable and hard to oxidize. Oxidation via sulfur was performed that readily gave the dithio product. Coordinating Gold(I) Chloride was successful and gave single and doubly coordinated Gold(I) Chloride.

3. Chapter 3 – Phosphorus (+1) Stabilization by Cyclic *N*-Heterocyclic Carbenes

3.1. Introduction

The Macdonald group was successful in synthesizing $[(^i\text{PrNHC}^{\text{Me}})_2\text{P}^{\text{I}}][\text{Cl}]$. In the previous chapter, other compounds of similar class have been synthesized and studied such as $[(^{\text{Me}}\text{NHC}^{\text{Me}})_2\text{P}^{\text{I}}][\text{Br}]$ and $[(^{\text{Et}}\text{NHC}^{\text{Me}})_2\text{P}^{\text{I}}][\text{Br}]$. The synthesis of such compounds were performed by optimizing the most effective protocol that we had previously developed.⁴² Again, although the direct reduction of PCl_3 using a sufficient excess of NHC does produce the desired product, the approach is not favoured mostly because it produces a chloroimidazolium chloride by-product which is hard to separate. However, it should also be noted that the procedure also wastes valuable NHC because at least one equivalent of carbene is sacrificed during the reduction. On the other hand, the ligand displacement approach incorporates all of the NHC into the desired product and generates only dppe that can be easily washed away with non-polar solvents such as pentane or toluene. Thus, the ligand displacement methodology is preferable, especially for NHC ligands that are difficult to prepare.

In this chapter chelating bis-carbene ligands are evaluated as ligands to stabilize P^{I} centers. Recently, stable biscarbenes have been synthesized^{33,64} such as the carbene 1,1'-dibenzyl-3,3'-methylenediimidazole-2,2'-diylidene (**Figure 3.1**). Given the foregoing discussion, we explore the use of ligand displacement from $[(\text{dppe})\text{P}^{\text{I}}]$ salts to prepare chelated bis-carbene adducts.

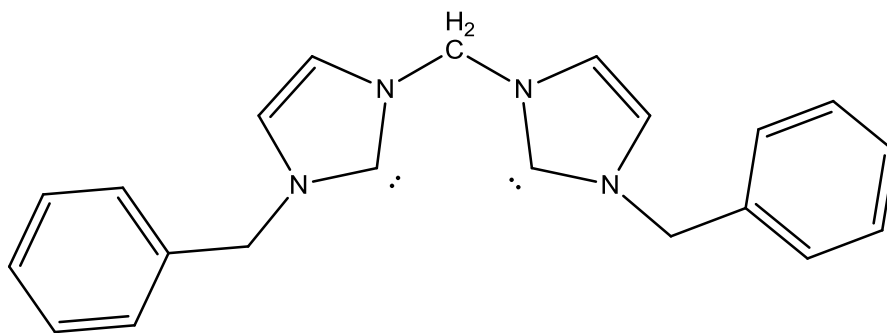


Figure 3.1: 1,1'-dibenzyl-3,3'-methylenediimidazole-2,2'-diylidene.

3.2. Experimental

General Procedures. All manipulations were carried out using standard inert atmosphere techniques. 1,2-bis(diphenylphosphino)ethane (dppe) was purchased from Strem Chemicals Inc. and all other chemicals and all other chemicals and reagents were obtained from Aldrich. All reagents were used without further purification. CD₃CN was dried over calcium hydride. All other solvents were dried on a series of Grubbs' type columns and were degassed prior to use.⁴⁷ Cyclic triphosphenium bromide ([dppeP^I][Br]),¹⁷ 1,1'-dibenzyl-3,3'-methylenediimidazole-2,2'-diylidene³³ and 1,1'-dimethyl-3,3'-methylenediimidazole-2,2'-diylidene⁶⁴ were all synthesized according to literature procedure. 1,1'-di-n-butyl-3,3'-methylenediimidazole-2,2'-diylidene was synthesized in a similar manner to the other two imidazolediylidenes.

Instrumentation. NMR spectra were recorded at room temperature in CD₃CN solutions on Bruker Avance III 500 MHz, Bruker Avance Ultrashield 300 MHz and Bruker Avance DPX 300 MHz spectrometers. Chemical shifts were reported in ppm relative to external standards (deuterated solvent for ¹H and ¹³C, 85% H₃PO₄ for ³¹P and CFCl₃ for ¹⁹F). Coupling constant magnitudes, |J|, are given in Hz. Melting point (Mp) or decomposition points (Dp) were obtained on samples sealed in glass capillaries under dry N₂ using an Electrothermal[®] Melting Point Apparatus. High resolution mass spectrometry and elemental analyses were performed by the University of Windsor Mass Spectrometry Service Laboratory using Micromass LCT and PerkinElmer 2400 combustion CHN analyser.

Theoretical Methods. All of the computational investigations were performed using the **Compute Canada Shared Hierarchical Academic Research Computing Network** (SHARCNET) facilities (www.sharcnet.ca) with the Gaussian09⁴⁸ program suite. Geometry optimizations have been calculated using density functional theory (DFT), specifically implementing the PBE1PBE method⁴⁹⁻⁵¹ in conjunction with the TZVP basis set⁵² for all atoms. The geometry optimizations were not subjected to any symmetry restrictions and each stationary point was confirmed to be a minimum having zero imaginary vibrational frequencies. Population analyses were conducted using the Natural Bond Orbital (NBO)⁵³ implementation included with the Gaussian package and the Atoms In Molecules (AIM) analyses⁵⁴ were conducted using AIM2000.^{55,56} Diagrams of calculated structures were generated using Gaussview 3.0.⁵⁷ Summaries of the optimized structures, including electronic energies and Cartesian components for each of the atoms, are detailed in the sections below.

Preparation of [(^{Bz}Bis)P^I][Br] (11)

To a colorless solution of 1,1'-dibenzyl-3,3'-methylenediimidazolium dibromide (150 mg, 0.306 mmol) in THF (20 mL) cooled in an acetone dry ice bath was added a colorless solution of K[N(SiMe₃)₂] (122 mg, 0.612 mmol) in THF (20 mL). The reaction flask was left to slowly warm up to -30 °C to give a pale yellow solution of 1,1'-dibenzyl-3,3'-methylenediimidazole-2,2'-diylidene. The filtrate was kept in an acetone dry ice bath throughout the filtration and to it was added [(dppe)P^I][Br] (120 mg, 0.236 mmol). The reaction was left to slowly warm up to room temperature and was allowed to stir for 1 hr. The orange precipitate was collected and washed with THF (3 x 20 mL) to

remove leftover dppe. The remaining volatiles were removed under reduced pressure to yield an orange product. Yield: 97% (100 mg, 0.228 mmol). $^{31}\text{P}\{^1\text{H}\}$ NMR (CD_3CN): -81.75 (s). ^1H NMR (CD_3CN): 5.07 (s, 4H, ArCH_2N), 5.94 (s, 2H, NCH_2N), 7.28-7.31 (m, 10H, CH_{Ar}), 7.39 (s, 2H, CH_{imid}), 7.41 (s, 2H, CH_{imid}). $^{13}\text{C}\{^1\text{H}\}$ NMR (CD_3CN): 51.62 (d, ArCH_2N , $^3J_{\text{CP}} = 10.87$), 59.53 (s, NCH_2N), 119.72 (s, CH_{imid}), 122.31 (s, CH_{imid}), 128.01, 128.66, 129.04 (s, ipso, ortho, meta Ar), 134.63 (s para Ar), 161.04 (d, PCN, $^1J_{\text{CP}} = 75.93$). Mp: 205 $^\circ\text{C}$ (dec.); Anal. Calc. for $\text{C}_{21}\text{H}_{20}\text{BrN}_4\text{P}$: C, 57.41; H, 4.59; N, 12.75. Found: C, 57.53; H, 4.75; N, 12.71. HRMS-ES Calc. for $\text{C}_{21}\text{H}_{20}\text{N}_4\text{P}^+$: 359.1425, Found: 359.1423.

Preparation of [$(^{\text{Me}}\text{Bis})\text{P}^{\text{I}}$][Br] (12)

To a colorless solution of 1,1'-dimethyl-3,3'-methylenediimidazolium dibromide (150 mg, 0.306 mmol) in THF (20 mL) cooled in an acetone dry ice bath was added a colorless solution of $\text{K}[\text{N}(\text{SiMe}_3)_2]$ (122 mg, 0.612 mmol) in THF (20 mL). The reaction flask was left to slowly warm up to -30 $^\circ\text{C}$ to give a pale yellow solution of 1,1'-dimethyl-3,3'-methylenediimidazole-2,2'-diylidene. The filtrate was kept in an acetone dry ice bath throughout the filtration and to it was added $[(\text{dppe})\text{P}^{\text{I}}][\text{Br}]$ (130 mg, 0.255 mmol). The reaction was left to slowly warm up to room temperature and was allowed to stir for 1 hr. The orange precipitate was collected and washed with THF (3 x 20 mL) to remove leftover dppe. The remaining volatiles were removed under reduced pressure to yield an orange product. Yield: 96% (70 mg, 0.244 mmol). $^{31}\text{P}\{^1\text{H}\}$ NMR (CDCl_3): -83.26 (s). ^1H NMR (CDCl_3): 3.61 (d, 6H, CH_3 , $^4J_{\text{PH}} = 0.9$), 6.66 (d, 2H, NCH_2N , $^4J_{\text{PH}} = 0.9$), 7.19 (m, CH_{imid} , $J = 1.9$), 7.83 (m, CH_{imid} , $J = 1.9$). $^{13}\text{C}\{^1\text{H}\}$ NMR (CDCl_3): 34.97 (d,

CH₃, ³J_{CP} = 11.3), 59.12 (s, NCH₂N), 119.93 (s, CH_{imid}), 122.65 (s, CH_{imid}), 160.94 (d, PCN, ¹J_{CP} = 76.9). Mp: 170-172 °C (dec.); Anal. Calc. for C₉H₁₂BrN₄P: C, 37.65; H, 4.21; N, 19.52. Found: C, 37.83; H, 4.32; N, 18.18. HRMS-ES-ES Calc. for C₉H₁₂N₄P⁺: 207.0800, Found: 207.0802.

Preparation of [(ⁿBuBis)P^I][Br] (13)

To a colorless solution of 1,1'-di-n-butyl-3,3'-methylenediimidazolium dibromide (150 mg, 0.355 mmol) in THF (20 mL) cooled in an acetone dry ice bath was added a colorless solution of K[N(SiMe₃)₂] (142 mg, 0.711 mmol) in THF (20 mL). The reaction flask was left to slowly warm up to -30 °C to give a pale yellow solution of 1,1'-di-n-butyl-3,3'-methylenediimidazole-2,2'-diylidene. The filtrate was kept in an acetone dry ice bath throughout the filtration and to it was added [(dppe)P^I][Br] (153 mg, 0.300 mmol). The reaction was left to slowly warm up to room temperature and was allowed to stir for 1 hr. The orange precipitate was collected and washed with THF (3 x 20 mL) to remove leftover dppe. The remaining volatiles were removed under reduced pressure to yield an orange product. Yield: 81% (90 mg, 0.242 mmol). ³¹P{¹H} NMR (CD₃CN): -83.07 (s). ¹H NMR (CD₃CN): 0.93 (t, 6H, CH₃, ³J_{HH} = 7.50), 1.33 (triplet of quartets, 4H, CH₂CH₂CH₃, ³J_{HH} = 7.50), 1.75 (pentet, 4H, CH₂CH₂CH₂, ³J_{HH} = 7.50), 3.87 (t, 4H, NCH₂CH₂, ³J_{HH} = 7.50), 5.99 (s, 2H NCH₂N), 7.24 (s, 2H, CH_{imid}), 7.36 (s, 2H, CH_{imid}). ¹³C{¹H} NMR (CD₃CN): 13.77 (s, CH₃), 20.19 (s, CH₂CH₂CH₃), 31.59 (s, CH₂CH₂CH₂), 48.99 (d, NCH₂CH₂, ³J_{CP} = 10.42), 60.23 (s, NCH₂N), 120.27 (s, CH_{imid}), 122.88 (s, CH_{imid}), 161.38 (d, PCN, ¹J_{CP} = 75.63). Mp: 155-156 °C (dec.); Anal. Calc. for

C₁₅H₂₄BrN₄P: C, 48.53; H, 6.51; N, 15.09. Found: C, 48.86; H, 6.39; N, 14.95. HRMS-ES-ES Calc. for C₁₅H₂₄N₄P⁺: 291.1739, Found: 291.1736.

Preparation of [(^{Bz}Bis)P^VS₂][Br] (14)

To an orange solution of [(^{Bz}Bis)P^I][Br] (10 mg, 0.023 mmol) in CD₃CN (5 mL) was added sulfur (S₈) (~2 mg, 0.008 mmol). The solution immediately lost its orange colour and showed a yellowish solution. After 10 minutes of sonication, an NMR was collected. ³¹P{¹H} NMR (CD₃CN): 18.82 (s). ¹H NMR (CD₃CN): 5.45 (s, 4H, ArCH₂N), 6.52 (s, 2H, NCH₂N), 7.42-7.49 (m, 10H, CH_{Ar}), 7.51 (s, 2H, CH_{imid}), 7.69 (s, 2H, CH_{imid}). ¹³C{¹H} NMR (CD₃CN): 53.24 (s, ArCH₂N), 60.90 (s, NCH₂N), 122.06 (s, CH_{imid}), 122.95 (s, CH_{imid}), 125.04, 129.63, 130.05 (s, ipso, ortho, meta Ar), 135.02 (s, para Ar), 143.47 (d, PC, ¹J_{CP} = 66.89). HRMS-ES-ES Calc. for C₂₁H₂₀N₄PS₂⁺: 423.0867, Found: 423.0872.

Preparation of [(^{Me}Bis)P^VS₂][Br] (15)

To an orange solution of [(^{Me}Bis)P^I][Br] (10 mg, 0.035 mmol) in CD₃CN (5 mL) was added sulfur (S₈) (~2.5 mg, 0.010 mmol). The solution immediately lost its orange colour and showed a yellowish solution. After 10 minutes of sonication, an NMR was collected. ³¹P{¹H} NMR (CDCl₃): 16.67 (s). ¹H NMR (CD₃CN): 4.24 (s, 6H, CH₃), 6.54 (d, 2H, NCH₂N, ⁴J_{HP} = 1.5), 7.52 (2H, d, CH_{imid}, ³J_{HH} = 2.1), 7.76 (d, 2H, CH_{imid}, ³J_{HH} = 2.1). ¹³C{¹H} NMR (CD₃CN): 38.18 (s, CH₃), 60.51 (s, NCH₂N), 121.75 (s, CH_{imid}), 126.88 (s, CH_{imid}), 149.52 (d, PCN, ¹J_{CP} = 65.74). HRMS-ES Calc. for C₉H₁₂N₄PS₂⁺: 271.0241, Found: 271.0242.

Preparation of [(ⁿBuBis)P^VS₂][Br] (16)

To an orange solution of [(ⁿBuBis)P^I][Br] (10 mg, 0.027 mmol) in CD₃CN (5 mL) was added sulfur (S₈) (~2 mg, 0.008 mmol). The solution immediately lost its orange colour and showed a yellowish solution. After 10 minutes of sonication, an NMR was collected. ³¹P{¹H} NMR (CD₃CN): 18.55 (s). ¹H NMR (CD₃CN): 0.97 (t, 6H, CH₃, ³J_{HH} = 7.50), 1.40 (triplet of quartets, 4H, CH₂CH₂CH₃, ³J_{HH} = 7.80), 1.99 (pentet, 4H, CH₂CH₂CH₂, ³J_{HH} = 7.50), 4.77 (t, 4H, NCH₂CH₂, ³J_{HH} = 7.50), 6.62 (d, 2H, NCH₂N, ⁴J_{HP} = 1.20), 7.52 (d, 2H, CH_{imid}, ⁴J_{HP} = 1.8), 7.76 (d, 2H, CH_{imid}, ⁴J_{HP} = 1.8). ¹³C{¹H} NMR (CD₃CN): 13.82 (s, CH₃), 20.12 (s, CH₂CH₂CH₃), 33.31 (s, CH₂CH₂CH₂), 50.76 (s, NCH₂CH₂), 60.51 (s, NCH₂N), 122.41 (s, CH_{imid}), 125.17 (s, CH_{imid}), 142.59 (d, PCN, ¹J_{CP} = 78.80). HRMS-ES Calc. for C₁₅H₂₄N₄PS₂⁺: 355.1180, Found: 355.1173.

3.3. Results and Discussions

3.3.1. Synthesis

The reaction of the acyclic NHCs with the triphosphenium P^I salt is somewhat straightforward and yields the desired $[(^R\text{NHC}^{R'})_2P^I][\text{Br}]$ product immediately and can be accomplished at room temperature. In contrast, the use of an analogous reaction protocol to obtain cyclic bis-NHC adducts has proven to be not as straightforward. The problem with the bis-NHC proligands is their increased sensitivity to temperature with respect to their non-chelating analogues. Presumably for this reason, the preparation of metal complexes with such chelating bis-NHC ligands are usually done in situ: the imidazolium salt precursor to the ligand, the base to generate the carbene and the metal center to be complexed are all mixed together to generate the product in situ rather than in a stepwise fashion. This approach works because the metal centers employed are stable in the presence of mild or strong bases.

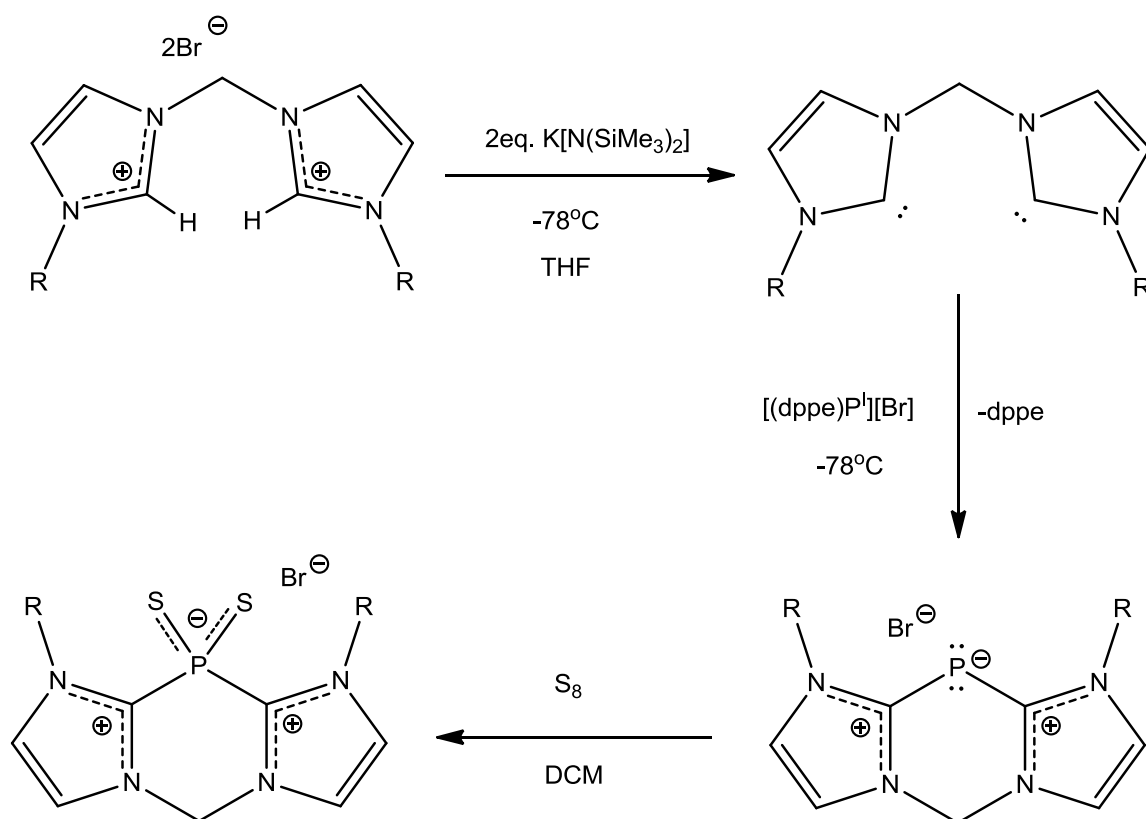
As for the triphosphenium P^I salt, the presence of a base in some cases causes the dppe to dissociate from the P^I center as evidenced by the signal at -12 ppm corresponding to free dppe observed in the ^{31}P NMR spectrum. Thus, it appeared as if a step wise reaction would be necessary, but such a protocol would require a biscarbene that is sufficiently stable at room temperature. Some groups were successful in isolating stable biscarbenes³³⁻³⁵, but in practice, as soon as the base is added to a solution of the imidazolium salt, the colour starts turning yellow (indicating the production of biscarbene) but the colour rapidly becomes red right away which indicates decomposition of the biscarbene. Because the addition of all ingredients at once does not give the

anticipated product, a step-wise protocol is followed. It would first require us to wait for the imidazolium deprotonation reaction to finish, filter off excess base and remove the other by-products salt (i.e. KBr) prior to the addition of the P^I source. In practice, this approach did not work because the biscarbene began to decompose as soon as it was synthesized and the work-up process generally resulted in the collection of products derived from the decomposed biscarbene.

However, Hermann and co-workers reported biscarbenes that were synthesized and successfully characterized at low temperatures.^{29,30} Thus, we reasoned that working with biscarbenes at low temperatures should allow us to utilize them in subsequent chemistry. Because of its ready preparation, the benzyl-substituted biscarbene ligand was examined first. Thus, the bis-imidazolium precursor was treated with potassium hexamethyldisilazide ($K[N(SiMe_3)_2]$) at $-78\text{ }^\circ\text{C}$. Deprotonation did not take place at that temperature but, upon warming to around $-30\text{ }^\circ\text{C}$, a yellow solution became apparent. At that point the reaction flask was cooled again to $-78\text{ }^\circ\text{C}$ in order to prevent the biscarbene from decomposing. Filtration was performed in an inert pre-cooled frit, where the filtrate was kept in an acetone bath to avoid decomposition of the biscarbene. Once filtration was complete, a cold solution of the $[(dppe)P^I][Br]$ was added in one portion and the reaction was allowed to warm up to room temperature and stirred for 1 hour. The targeted salt $[Biscarbene-P^I][Br]$ was collected via filtration and washed with THF to remove any leftover dppe. As with the acyclic compounds described in Chapter 2, we probed some of the oxidation chemistry of these chelated compounds. In particular, the oxidation reactions with sulfur were done on an NMR scale, where sulfur is added directly to $[Biscarbene-P^I][Br]$ in CD_3CN to give the dithio P^V adduct. The general synthesis of the

[Biscarbene- P^I][Br $^-$] and its subsequent oxidation with sulfur are illustrated in **Scheme**

3.1.



Scheme 3.1: synthesis of $[Biscarbene-P^I][Br^-]$ and its subsequent oxidation with sulfur.

3.3.2. NMR Analysis

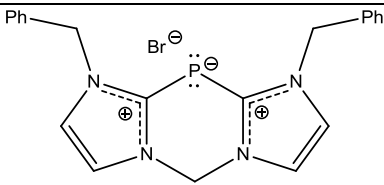
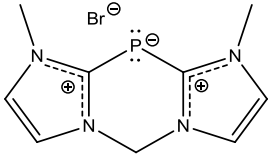
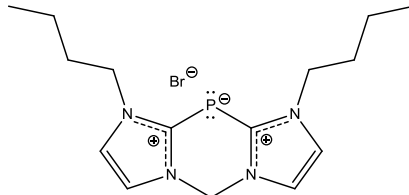
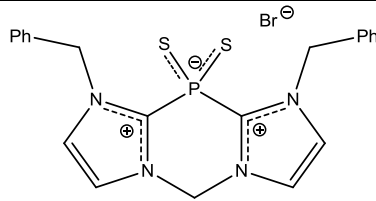
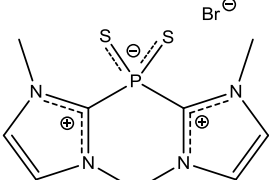
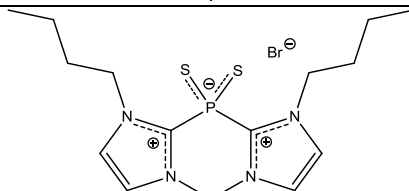
Structure	Compound	δ^a
	$[(^{\text{Bz}}\text{Bis})\text{P}^{\text{I}}][\text{Br}]$ (11)	-81.8
	$[(^{\text{Me}}\text{Bis})\text{P}^{\text{I}}][\text{Br}]$ (12)	-83.3
	$[(^{\text{nBu}}\text{Bis})\text{P}^{\text{I}}][\text{Br}]$ (13)	-83.1
	$[(^{\text{Bz}}\text{Bis})\text{P}^{\text{V}}\text{S}_2][\text{Br}]$ (14)	18.8
	$[(^{\text{Me}}\text{Bis})\text{P}^{\text{V}}\text{S}_2][\text{Br}]$ (15)	16.7
	$[(^{\text{nBu}}\text{Bis})\text{P}^{\text{V}}\text{S}_2][\text{Br}]$ (16)	18.6

Table 3.1: Structures and ^{31}P NMR data of cyclic $[(^{\text{R}}\text{Bis})\text{P}^{\text{I}}][\text{Br}]$ salts and their oxidized variants.

All of the desired chelated bis-carbene adducts, namely $[(^{\text{Bz}}\text{Bis})\text{P}^{\text{I}}][\text{Br}]$ (**11**), $[(^{\text{Me}}\text{Bis})\text{P}^{\text{I}}][\text{Br}]$ (**12**) and $[(^{\text{nBu}}\text{Bis})\text{P}^{\text{I}}][\text{Br}]$ (**13**) were produced in high yields using the

methodology described above. In all cases, the imidazolium salt precursor was in slight excess to the P^I source to ensure complete ligand displacement of the triphosphenium salt. We reasoned that any excess carbene would decompose and be washed away along with the leftover dppe using THF and the high yields and purity are consistent with that postulate. The ^{31}P NMR of **11**, **12** and **13** are very similar: -81.8 ppm, -83.3 ppm and -83.1 ppm respectively. Comparing these chemical shifts to the ones observed in the acyclic compounds, these chemical shifts are considerably deshielded. Furthermore, in contrast to the acyclic analogues, we do not observe a significant difference in the chemical shift of the methyl-substituted variant. Thus it appears as if the presence of the bridging methylene group enforces a common geometry (as we had anticipated) that is less affected by the identity of the terminal substituents. It is also worth noting that the more shielded signals are consistent with a more co-planar (and π -delocalized) structure for the chelated P^I cations.⁶⁵

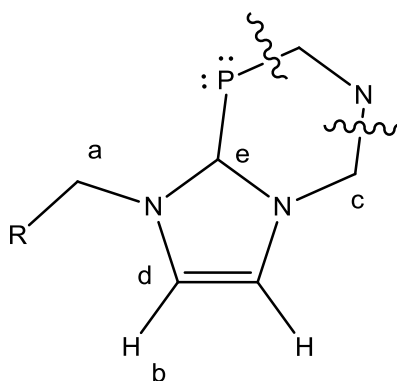


Figure 3.2: Labeling of protons and carbons.

The 1H NMR spectrum for **11** showed the aromatic peaks where they would be expected. The backbone protons were buried under the aromatic multiplet, but the

integration confirmed the presence of 4 protons that would correspond to the backbone protons. The bridging CH₂ in this case appears as a singlet. As for **12**, the proton NMR was not easily assigned. The CH₃ as well as the bridging protons produce doublets while the protons on the backbone showed triplets. The signals for the terminal CH₃ and the bridging protons both have coupling of 0.9 Hz but are certainly not coupled to each other. If they were coupled to each other, then one would see a triplet for the CH₃ and a quartet for the bridging CH₂. However, both signals are doublets with nearly identical coupling constants which implies a ⁴J_{HP} coupling of the protons to the phosphorus nucleus. The "triplet" signals observed for the backbone hydrogen atoms come from the two protons coupling to each other as well as coupling to phosphorus which gives a doublet of doublets that appear as a triplet due to the similar coupling constant of the ⁴J_{HP} and the ³J_{HH}. For **13**, the bridging CH₂ and the backbone protons were singlets unlike compound **12**. The "sextet" signals in the spectrum are actually a triplet of quartets in which the ³J_{HH} constants are similar in magnitude;; the protons are coupling to the neighboring CH₂ and CH₃ giving this sextet pattern than the expected pentet pattern that would be expected for organic aliphatic chains. Looking at intensity patterns, one realizes that the intensity of the multiplet pattern is 1:3:4:4:3:1 which is appropriate to a triplet of quartets than a normal sextet (a normal sextet arising from a spin half system would require a 1:5:10:10:5:1 pattern).

The analysis of the ¹³C NMR spectra of these compounds is very similar to that of the acyclic systems. Most instructively, each carbon atom attached to the phosphorus has a doublet from coupling to phosphorus with a ¹J_{CP} of about 75 Hz for all three compounds.

Oxidation of these compounds with sulfur was straightforward and always produces the di-thio P^V products regardless of the stoichiometry used (**Scheme 3.1**). The formation of the oxidized product was readily detected by ^{31}P NMR spectroscopy in which the chemical shift at ca. -83 ppm disappears and another peak appears at ca. $+18$ ppm. As with the acyclic variants examined in Chapter 2, the 1H and ^{13}C NMR spectra are similar to those of the un-oxidized starting compounds. Upon filtration of the excess sulfur, the resultant filtrate is colourless. Just as was the case with the acyclic system, the chromophore of these compounds gives it its orange colour that is lost upon oxidation of the molecules.

3.3.3. Mass Spec Analysis

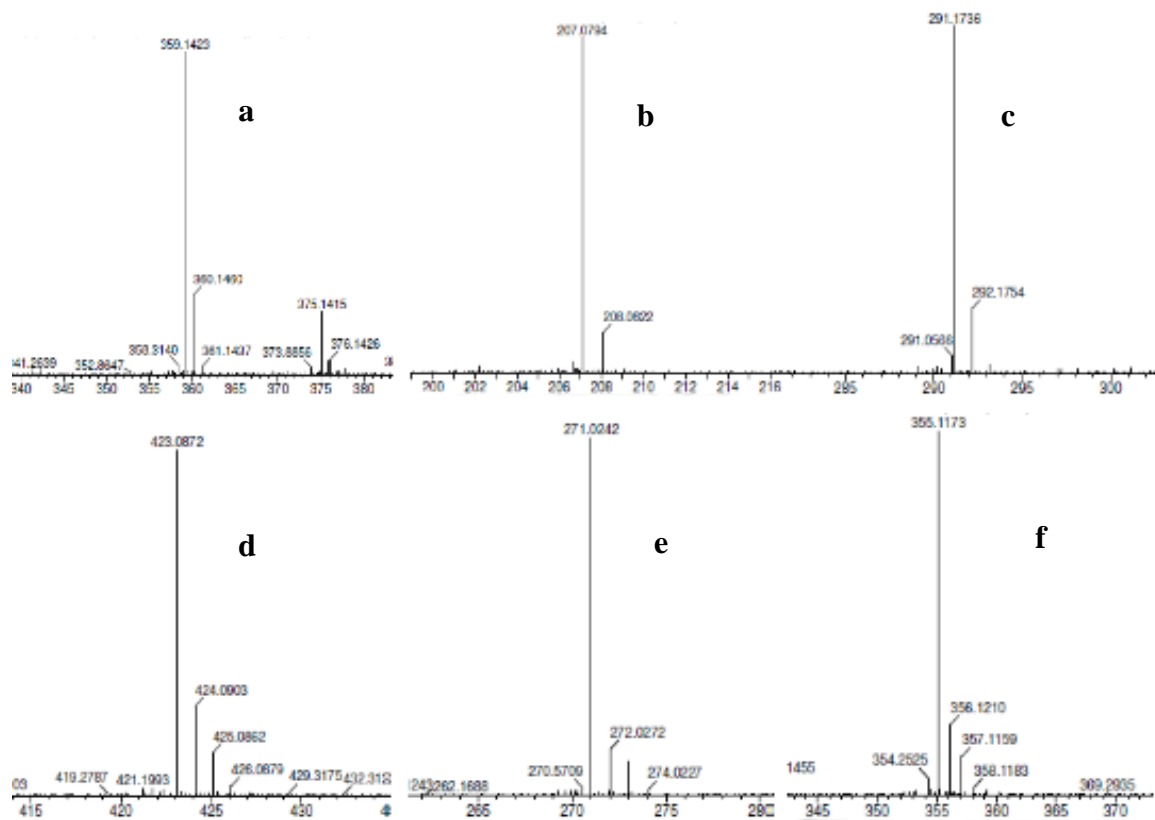


Figure 3.3: Mass Spectra of **11-16**. (Electrospray ionization)

Unfortunately, no crystalline samples suitable for analysis by X-ray diffraction were obtained for any of the compounds synthesized in this chapter, but High Resolution Mass Spec (HRMS-ES) was performed on all samples to confirm the composition of the materials. The molecular formula predicted for **11** is $C_{21}H_{20}N_4P^+$; its calculated molecular weight is 359.1425 Da and the observed m/z value was 359.1423 Da (**Figure 3.3a**). The oxidized di-thio derivatives of the compound ($C_{21}H_{20}N_4PS_2^+$), **14**, has a calculated molecular weight of 423.0867 Da and the observed m/z value found was 423.0872 Da

(**Figure 3.3d**). As for **12**, the calculated and found m/z values for $C_9H_{12}N_4P^+$ were 207.0800 Da and 207.0802 Da respectively (**Figure 3.3b**). Its di-thio variant (**15**) was calculated to be 271.0241Da for $C_9H_{12}N_4PS_2^+$ and the value observed was 271.0242 Da (**Figure 3.3e**). As for the n-butyl carbene adduct, **13**, the calculated and found m/z values for $C_{15}H_{24}N_4P^+$ were 291.1739 Da and 291.1736 Da (**Figure 3.3c**) respectively. The m/z value for its sulfur oxidized variant (**16**) was calculated to be 355.1180 Da for $C_{15}H_{24}N_4PS_2^+$ and the value observed was 355.1173 Da (**Figure 3.3f**).

Molecular Formula	Calculated (Da)	Found (Da)*
$C_{21}H_{20}N_4P^+$	359.1425	359.1423
$C_9H_{12}N_4P^+$	207.0800	207.0802
$C_{15}H_{24}N_4P^+$	291.1739	291.1736
$C_{21}H_{20}N_4PS_2^+$	423.0867	423.0872
$C_9H_{12}N_4PS_2^+$	271.0241	271.0242
$C_{15}H_{24}N_4PS_2^+$	355.1180	355.1173

*(Electrospray Method)

Table 3.2: Calculated and found Mass Spec values for **11-16**.

3.3.4. Computational Studies

As with the acyclic structures presented in Chapter 2, DFT computational studies were performed on the cyclic structures to further study the bonding, electronics and structure of these compounds.

Compound	C–P Bond Distance (Å)	C–P–C Bond Angle (°)	N–C–P–C Dihedral Angle (°)
11'	1.79896, 1.79676	91.48	21.35 – 21.47
12'	1.79508, 1.79507	91.73	19.07 – 19.07
13'	1.79427, 1.79428	92.32	15.75 – 15.75
14'	1.87577, 1.87579 P–S: 1.95084	91.62	34.37 – 34.37
15'	1.87000, 1.87000 P–S: 1.95910	91.28	32.40 – 32.39
16'	1.87469, 1.87475 P–S: 1.95173	91.52	33.33 – 33.35

Table 3.3: Bond distances and angles. DFT (PBE1PBE/TZVP)

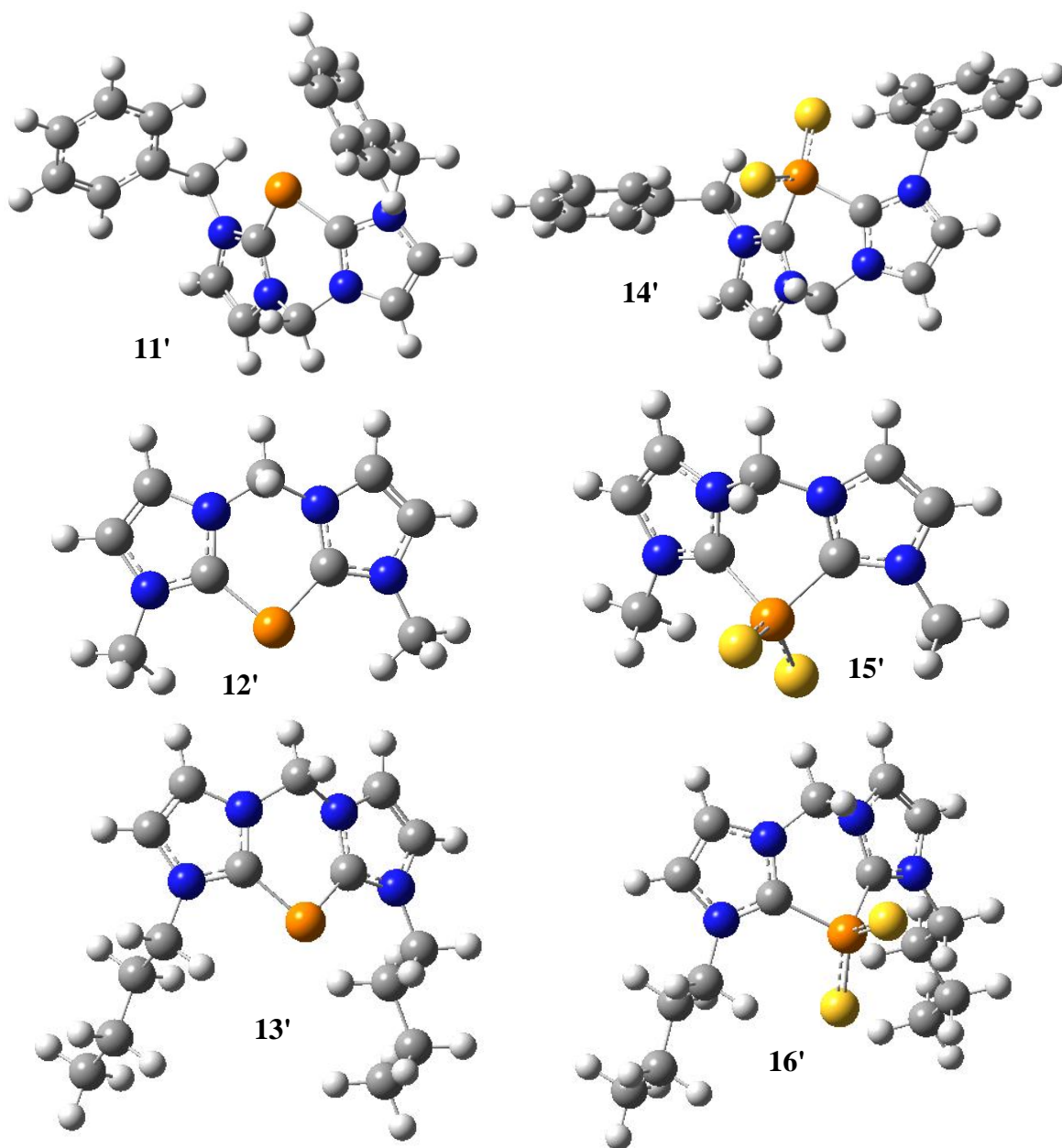


Figure 3.4: Geometry-optimized structures for model compounds **11'-16'**. DFT (PBE1PBE/TZVP)

Examination of the C–P bond distances (**Table 3.3**) for the optimized model structures shows that the three compounds are very comparable which confirms that the

terminal R group on the nitrogen atoms has a much smaller effect on the C–P bond distance with respect to the acyclic analogues. In the acyclic system the C–P bond distance for **1'** was about 1.81 and 1.84 for **9'** and **10'**. In the cyclic system the C–P bond distance for compounds **11'-13'** is between 1.79 and 1.80, which are notably shorter than what is observed in the acyclic systems. This suggests that there is a greater interaction between the second lone pair on the phosphorus atom and the π -system of the molecule which would produce stronger bonding. This supposition is examined in further detail below.

Compound	Symmetry	HOMO (eV)	LUMO (eV)	HOMO-LUMO Gap (eV)
11'	C ₁	−8.58	−0.15	4.62
12'	C ₁	−8.87	−0.16	4.61
13'	C ₁	−8.61	−0.15	4.56
14'	C ₁	−9.45	−0.18	4.54
15'	C ₁	−9.63	−0.19	4.47
16'	C ₁	−9.46	−0.18	4.51

Table 3.4: Energy gap calculations. DFT (PBE1PBE/TZVP)

In terms of the electronic structures of the model compounds, it is apparent that the HOMO-LUMO gaps of the oxidized compounds are smaller than those of their unoxidized counterparts. This behavior is different from the acyclic systems, in which oxidation of the acyclic system resulted in a larger HOMO-LUMO gap and suggests that

there may be significant chemical differences possible between the cyclic and acyclic variants.

Compound	Charge on Phosphorus	P–C WBI	C–N WBI	C–N WBI
11'	0.27166	1.1271	1.2366	1.1910
12'	0.25609	1.1294	1.2429	1.1922
13'	0.24800	1.1319	1.2455	1.1888
14'	0.97780	0.6996	1.3296	1.2490
15'	0.97066	0.6938	1.3180	1.2533
16'	0.97461	0.6964	1.3270	1.2495

Table 3.5: NBO WBI values for the model complexes. DFT (PBE1PBE/TZVP)

The Wiberg Bond Indices (WBI) of these structures provide additional insight into the nature of the P–C bonding of the oxidized and un-oxidized within these models. In the un-oxidized compounds **11'**, **12'** and **13'**, the bond order is greater than one which suggests the presence of conjugation in the P–C bond. In the acyclic system, this number was about 1.05 for **9'** and **10'** and 1.09 for **1'**. In the cyclic system, the number is about 1.13 for compounds **11'**-**13'** which is significantly greater. This considerable increase in the bond order is consistent with the shorter P–C bond distance observed in the cyclic compounds and is almost certainly a consequence of the geometric constraints of the chelate. As for the oxidized model compounds **14'**-**16'**, the bond order significantly decreases to just under 0.7 for the three compounds. Comparing the C–N bond orders of

the cyclic and acyclic systems, one can see that in the acyclic system, the two values of the C–N bond order almost identical to each other, while the C–N bond orders within an individual heterocycle in the chelated system differ significantly. This is readily understood because the two nitrogen atoms have different R groups, one of which is the connecting CH₂ bridge. Furthermore, whereas oxidizing the acyclic systems with S doesn't change the C–N bond order considerably, in the cyclic system the C–N bond order does change significantly, where it increases upon oxidizing the phosphorus center. Again, all of these features are consistent with the presence of greater π -delocalization in the chelate complexes with respect to the acyclic analogues.

Compound	1 st Lone Pair Population on Phosphorus	2 nd Lone Pair Population on Phosphorus	1 st Lone Pair Population on Nitrogen	2 nd Lone Pair Population on Nitrogen	Interaction of 2 nd Lone Pair of Phosphorus with C–N bond (kcal/mol)
11'	1.94802	N/A [*]	1.52574	1.57038	N/A [*]
12'	1.94978	1.43167	1.57125	1.57125	96.54, 96.54
13'	1.94792	1.43552	1.57439	1.57440	97.76, 97.76
14'	N/A	N/A	1.53414	1.46679	N/A
15'	N/A	N/A	1.53107	1.53108	N/A
16'	N/A	N/A	1.53364	1.53367	N/A

^{*}Calculations showed that the second lone pair is better described as a π bond than a lone pair.

Table 3.6: Lone pair population and interaction. DFT (PBE1PBE/TZVP)

In order to further elucidate the role played by the second lone pair of the phosphorus in the π -system of the parent (un-oxidized) compounds, the population and

interactions of the second lone pair have been calculated. In terms of electron population, the first lone pair shows a population of about 1.95 which shows minimal contribution to the π -system of the molecule and is clearly of σ -type symmetry; however, the second lone pair has a population of about 1.4 for **12** and **13**, which shows significant delocalization of the lone pair into the π -system of the molecule. In fact, for the model **11'**, the analyses suggests that the second lone pair is better described as being a π bond between P and C rather than a lone pair. Given all the foregoing discussion, it is not surprising that the population of ca. 1.4 is significantly smaller than the corresponding values observed in the acyclic system. In fact, the energetic stabilization associated with the interaction between the lone pair and the adjacent C–N bond in the π -system is as high as 97 kcal/mol in the cyclic models as compared to 32 and 62 in the acyclic system.

Compound	$\lambda_1/\lambda_{\text{max}}$ (nm)	λ_2 (nm)	λ_3 (nm)	λ_4 (nm)
11'	333.51	278.07	269.63	–
12'	332.49	318.20	265.37	261.84
13'	338.66	269.84	248.63	–
14'	347.66	345.33	338.56	321.64
15'	353.48	348.21	343.70	321.90
16'	351.39	346.15	335.35	316.14

Table 3.7: Time dependent (TD) calculations. TD-DFT (PBE1PBE/TZVP)

The parent cyclic compounds are orange in colour, while the oxidized di-thio compounds are pale yellow. As explained in Chapter 2, a greater extent of π -conjugation

in a system leads to a lower HOMO-LUMO gap and thus, a lower energy required for excitation of an electron.

The data in **Table 3.4** suggest that, unlike the acyclic system, the cyclic system has a lower HOMO-LUMO gap in the oxidized compounds than in the un-oxidized ones. **Table 3.7** shows the wavelength values of the oxidized and un-oxidized compounds and confirms the observation in the HOMO-LUMO gap difference between the two where the oxidized system has a lower wavelength value.

4. Conclusions and Future Work

4.1. Conclusions

The main focus of this project was the stabilization of phosphorus in the unusually low (+1) oxidation state. This univalent phosphorus, P^I , is very electron rich which gives it a very different reactivity than its +3 and +5 oxidation state analogues. Our research group previously reported several approaches to the synthesis of base-stabilized univalent phosphorus halide reagents containing cations such as $[(dppe)P^I][Br]$.¹⁵⁻¹⁷ Furthermore, we discovered that the reaction of two equivalents of *N*-heterocyclic carbenes (NHCs) with such P^I salts produces salts containing $[(^R\text{NHC}^{R'})_2P^I]^+$ cations through a ligand replacement mechanism in which the weaker phosphine ligands are displaced by the stronger NHC donors.⁴²

Various derivatives of these acyclic $[(^R\text{NHC}^{R'})_2P^I]^+$ cations containing different R groups (Me and Et) and different anions such as triflate (OTf) and tetraphenylborate (BPh₄) have been synthesized. Other cyclic carbenes have also been used in the synthesis of stable P^I cations. Oxidation reactions have been performed to study the reactivity of these P^I cations and their metal coordination ability. Different computational studies have been performed to study the bonding, electronics and structure of these compounds.

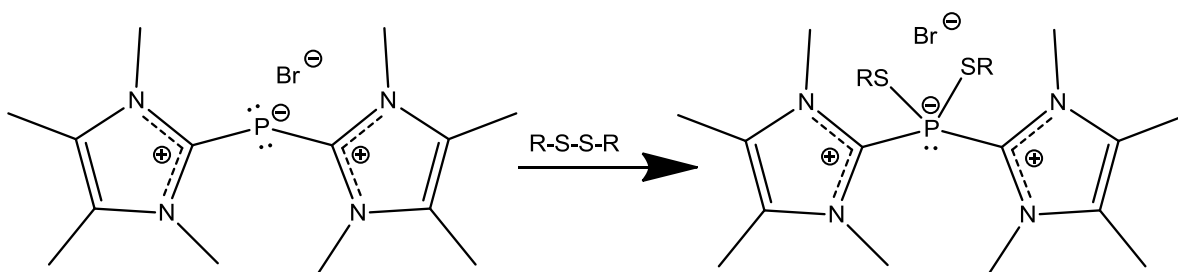
Overall, the work demonstrated the viability of this improved approach toward the preparation of dye-like molecules containing low-valent phosphorus. The studies also confirmed that cyclic dyes derived from chelating bis-carbene ligands can be prepared in very high yield. The experimental observations and computational work identifies some

significant differences between the acyclic and cyclic dyes that may be of use in the future.

4.2. Future Work

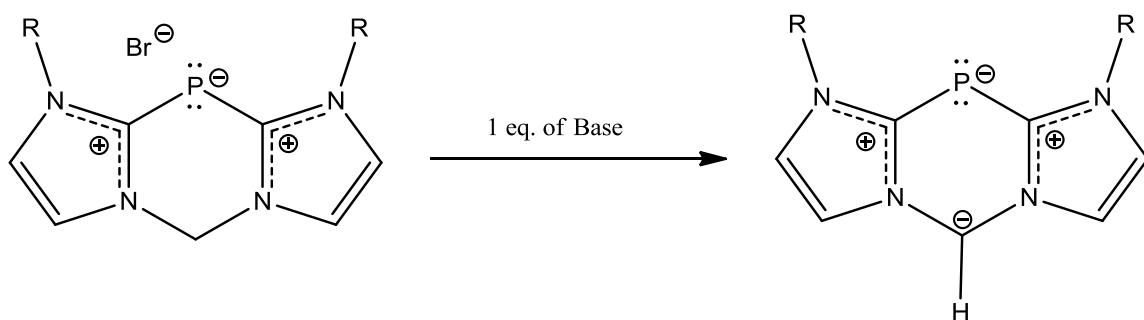
The research presented in this dissertation will further be investigated at different levels as the work done inspired new ideas in stabilization of P^I cations and the reactivity of such cations.

As for the acyclic system, other oxidation reactions can be examined such as reacting $[(NHC_2)P^I]^+$ with a disulfide which can be useful in biological dye applications if successful (**Scheme 4.1**). The successful coordination of two equivalents of gold by the acyclic compounds is a very interesting result that could be developed for catalytic purposes.⁶⁶ Other reactions that can be tried with the acyclic system include investigating the coordination chemistry of the P^I cations with metal centers other than gold. For example, the reaction of $[(NHC_2)P^I]^+$ with Wilkinson's catalyst (Tris(triphenylphosphine)rhodium(I) Chloride) resulted in a complicated ^{31}P NMR spectrum showing second order coupling along with a peak that corresponds to the free triphenylphosphine ligand. These preliminary observations should be pursued in much more detail.



Scheme 4.1: Reacting $[(^MeNHC^Me)_2P^I][Br]$ with a disulfide.

For the cyclic system, other oxidation reactions can be performed just as the case with the acyclic system to study the chemistry of these cyclic systems. Another reaction that can be performed is the single deprotonation of the bridging CH_2 to give a connecting CH^- fragment that will give an overall neutral molecule (**Scheme 4.2**). Having a neutral overall molecule will allow it to be soluble in many organic solvents which will be easier to handle and very interesting to study. Another idea that is to be considered is trying a different linker such as BR_2 which will give an overall neutral molecule without the need of deprotonating it. Such linked carbenes have been synthesized and the BPh_2 carbene have been tried without any success yet. The BH_2 seems more promising, but the synthesis of the BH_2 biscarbene seems to be more challenging than described in literature.^{32,35}



Scheme 4.2: Reacting $[(^{\text{R}}\text{Bis})\text{P}^{\text{I}}][\text{Br}]$ with an equivalence of base to give the neutral overall compound shown with a connecting CH^- fragment.

5. References

- (1) Fluck, E. *Pure Appl. Chem.* **1988**, 60, 431.
- (2) Arduengo, A. J.; Stewart, C. A.; Davidson, F.; Dixon, D. A.; Becker, J. Y.; Culley, S. A.; Mizen, M. B. *J. Am. Chem. Soc.* **1987**, 109, 627.
- (3) Jensen, W. B. *J. Chem. Educ.* **2007**, 84, 1418.
- (4) Parkin, G. *J. Chem. Educ.* **2006**, 83, 791.
- (5) McNaught A. D.; Wilkinson, A. *IUPAC Gold Book*; IUPAC, 1997.
- (6) Ellis, B. D.; Macdonald, C. L. B. *Coord. Chem. Rev.* **2007**, 251, 936.
- (7) Schmidpeter, A.; Lochschmidt, S.; Sheldrick, W. S. *Angew. Chem. Int. Ed. Engl.* **1982**, 21, 63.
- (8) Schmidpeter, A.; Lochschmidt, S.; Karaghiosoff, K.; Sheldrick, W. S. *J. Chem. Soc., Chem. Commun.* **1985**, 0, 1447.
- (9) Schmidpeter, A.; Lochschmidt, S.; Sheldrick, W. S. *Angew. Chem. Int. Ed. Engl.* **1985**, 24, 226.
- (10) Schmidpeter, A.; Lochschmidt, S. *Angew. Chem. Int. Ed. Engl.* **1986**, 25, 253.
- (11) Boon, J. A.; Byers, H. L.; Dillon, K. B.; Goeta, A. E.; Longbottom, D. A. *Heteroat. Chem.* **2000**, 11, 226.
- (12) Barnham, R. J.; Deng, R. M. K.; Dillon, K. B.; Goeta, A. E.; Howard, J. A. K.; Puschmann, H. *Heteroat. Chem.* **2001**, 12, 501.
- (13) Dillon, K. B.; Monks, P. K.; Olivey, R. J.; Karsch, H. H. *Heteroat. Chem.* **2004**, 15, 464.
- (14) Burton, J. D.; Deng, R. M. K.; Dillon, K. B.; Monks, P. K.; J. Olivey, R. *Heteroat. Chem.* **2005**, 16, 447.
- (15) Ellis, B. D.; Carlesimo, M.; Macdonald, C. L. B. *Chem. Commun. (Cambridge, U. K.)* **2003**, 0, 1946.
- (16) Ellis, B. D.; Macdonald, C. L. B. *Inorg. Chem.* **2006**, 45, 6864.
- (17) Norton, E. L.; Szekeley, K. L. S.; Dube, J. W.; Bomben, P. G.; Macdonald, C. L. B. *Inorg. Chem.* **2008**, 47, 1196.
- (18) Kilian, P.; Slawin, A. M. Z.; Woollins, J. D. *Dalton Trans.* **2006**, 0, 2175.
- (19) Driess, M.; Aust, J.; Merz, K.; van Wüllen, C. *Angew. Chem. Int. Ed.* **1999**, 38, 3677.
- (20) Bourissou, D.; Guerret, O.; Gabbai, F. P.; Bertrand, G. *Chem. Rev. (Washington, DC, U. S.)* **1999**, 100, 39.
- (21) Irikura, K. K.; Goddard, W. A.; Beauchamp, J. L. *J. Am. Chem. Soc.* **1992**, 114, 48.
- (22) Arduengo, A. J.; Dias, H. V. R.; Harlow, R. L.; Kline, M. *J. Am. Chem. Soc.* **1992**, 114, 5530.
- (23) Fischer, E. O.; Maasböl, A. *Angew. Chem. Int. Ed. Engl.* **1964**, 3, 580.
- (24) Arduengo, A. J.; Harlow, R. L.; Kline, M. *J. Am. Chem. Soc.* **1991**, 113, 361.
- (25) Wanzlick, H. W.; Schikora, E. *Angew. Chem.* **1960**, 72, 494.
- (26) Sch önherr, H.-J.; Wanzlick, H.-W. *Chem. Ber.* **1970**, 103, 1037.
- (27) Kuhn, N.; Kratz, T. *Synthesis* **1993**, 1993, 561.
- (28) Igau, A.; Grutzmacher, H.; Baceiredo, A.; Bertrand, G. *J. Am. Chem. Soc.* **1988**, 110, 6463.

- (29) Herrmann, W. A.; Köcher, C.; Gooßen, L. J.; Artus, G. R. J. *Chemistry – A European Journal* **1996**, *2*, 1627.
- (30) Herrmann, W. A.; Elison, M.; Fischer, J.; Köcher, C.; Artus, G. R. J. *Chemistry – A European Journal* **1996**, *2*, 772.
- (31) Caballero, A. n.; Díez-Barra, E.; Jalón, F. A.; Merino, S.; Tejeda, J. J. *Organomet. Chem.* **2001**, *617–618*, 395.
- (32) Danopoulos, A. A.; Winston, S.; Motherwell, W. B. *Chem. Commun. (Cambridge, U. K.)* **2002**, *0*, 1376.
- (33) Paulose, T. A. P.; Wu, S.-C.; Olson, J. A.; Chau, T.; Theaker, N.; Hassler, M.; Quail, J. W.; Foley, S. R. *Dalton Trans.* **2012**, *41*, 251.
- (34) Nieto, I.; Bontchev, R. P.; Smith, J. M. *Eur. J. Inorg. Chem.* **2008**, *2008*, 2476.
- (35) Shishkov, I. V.; Rominger, F.; Hofmann, P. *Organometallics* **2009**, *28*, 3532.
- (36) Dimroth, K.; Hoffmann, P. *Angew. Chem. Int. Ed. Engl.* **1964**, *3*, 384.
- (37) Allmann, R. *Chem. Ber.* **1966**, *99*, 1332.
- (38) Dimroth, K.; Hoffmann, P. *Chem. Ber.* **1966**, *99*, 1325.
- (39) Jutzi, P. *Angew. Chem. Int. Ed. Engl.* **1975**, *14*, 232.
- (40) Huang, J.; Stevens, E. D.; Nolan, S. P.; Petersen, J. L. *J. Am. Chem. Soc.* **1999**, *121*, 2674.
- (41) Schmidpeter, A.; Lochschmidt, S.; Willhalm, A. *Angew. Chem. Int. Ed. Engl.* **1983**, *22*, 545.
- (42) Ellis, B. D.; Dyker, C. A.; Decken, A.; Macdonald, C. L. B. *Chem. Commun. (Cambridge, U. K.)* **2005**, *0*, 1965.
- (43) Masuda, J. D.; Schoeller, W. W.; Donnadieu, B.; Bertrand, G. *Angew. Chem. Int. Ed.* **2007**, *46*, 7052.
- (44) Masuda, J. D.; Schoeller, W. W.; Donnadieu, B.; Bertrand, G. *J. Am. Chem. Soc.* **2007**, *129*, 14180.
- (45) Back, O.; Kuchenbeiser, G.; Donnadieu, B.; Bertrand, G. *Angew. Chem. Int. Ed.* **2009**, *48*, 5530.
- (46) Gomez-Ruiz, S.; Hey-Hawkins, E. *New J. Chem.* **2010**, *34*, 1525.
- (47) Pangborn, A. B.; Giardello, M. A.; Grubbs, R. H.; Rosen, R. K.; Timmers, F. J. *Organometallics* **1996**, *15*, 1518.
- (48) Frisch, M. J.; Trucks, G. W.; Schlegel, H. B.; Scuseria, G. E.; Robb, M. A.; Cheeseman, J. R.; Scalmani, G.; Barone, V.; Mennucci, B.; Petersson, G. A.; Nakatsuji, H.; Caricato, M.; Li, X.; Hratchian, H. P.; Izmaylov, A. F.; Bloino, J.; Zheng, G.; Sonnenberg, J. L.; Hada, M.; Ehara, M.; Toyota, K.; Fukuda, R.; Hasegawa, J.; Ishida, M.; Nakajima, T.; Honda, Y.; Kitao, O.; Nakai, H.; Vreven, T.; Montgomery, J., J. A.; Peralta, J. E.; Ogliaro, F.; Bearpark, M.; Heyd, J. J.; Brothers, E.; Kudin, K. N.; Staroverov, V. N.; Kobayashi, R.; Normand, J.; Raghavachari, K.; Rendell, A.; Burant, J. C.; Iyengar, S. S.; Tomasi, J.; Cossi, M.; Rega, N.; Millam, N. J.; Klene, M.; Knox, J. E.; Cross, J. B.; Bakken, V.; Adamo, C.; Jaramillo, J.; Gomperts, R.; Stratmann, R. E.; Yazyev, O.; Austin, A. J.; Cammi, R.; Pomelli, C.; Ochterski, J. W.; Martin, R. L.; Morokuma, K.; Zakrzewski, V. G.; Voth, G. A.; Salvador, P.; Dannenberg, J. J.; Dapprich, S.; Daniels, A. D.; Farkas, Ö.; Foresman, J. B.; Ortiz, J. V.; Cioslowski, J.; Fox, D. J.; Gaussian, Inc.: Wallingford CT, 2009.
- (49) Perdew, J. P.; Burke, K.; Ernzerhof, M. *Phys. Rev. Lett.* **1997**, *78*, 1396.
- (50) Adamo, C.; Barone, V. *The Journal of Chemical Physics* **1999**, *110*, 6158.

- (51) Perdew, J. P.; Burke, K.; Ernzerhof, M. *Phys. Rev. Lett.* **1996**, 77, 3865.
- (52) Schafer, A.; Huber, C.; Ahlrichs, R. *J. Chem. Phys.* **1994**, 100, 5829.
- (53) Reed, A. E.; Curtiss, L. A.; Weinhold, F. *Chem. Rev.* **1988**, 88, 899.
- (54) Bader, R. F. W. *Chem. Rev.* **1991**, 91, 893.
- (55) Biegler-Konig, F.; Schonbohm, J. *J. Comput. Chem.* **2002**, 23, 1489.
- (56) Biegler-Konig, F.; Schonbohm, J.; Bayles, D. *J. Comput. Chem.* **2001**, 22, 545.
- (57) Gaussian Inc.: Pittsburgh, PA, 2003.
- (58) SMART Bruker AXS Inc.: Madison, WI, 2001.
- (59) SAINTPlus Bruker AXS Inc.: Madison, WI, 2001.
- (60) SADABS Bruker AXS Inc.: Madison, WI, 2001.
- (61) Altomare, A., Burla, M. C., Camalli, M., Cascarano, G., Giacovazzo, C., Guagliardi, A. G. G., Moliterni, G., Polidori, G., Spagna, R. *J. Appl. Crystallogr.* **1999**, 32, 115.
- (62) Sheldrick, G. M. *Acta Crystallographica Section A* **2008**, 64, 112.
- (63) Farrugia, L. J. *J. Appl. Crystallogr.* **1999**, 32, 837.
- (64) Wells, K. D.; Ferguson, M. J.; McDonald, R.; Cowie, M. *Organometallics* **2008**, 27, 691.
- (65) Back, O.; Henry-Ellinger, M.; Martin, C. D.; Martin, D.; Bertrand, G. *Angew. Chem. Int. Ed.* **2013**, 52, 2939.
- (66) Dube, J. W.; Macdonald, C. L. B.; Ragogna, P. J. *Angew. Chem. Int. Ed.* **2012**, 51, 13026.

Vita Auctoris

NAME: Ala'aeddeen Swidan

PLACE OF BIRTH: Amman, Jordan

YEAR OF BIRTH: 1989

EDUCATION: J. L. Forster Secondary School, Windsor, ON, 2007

University of Windsor, B.Sc., Windsor, ON, 2011

University of Windsor, M.Sc., Windsor, ON, 2013